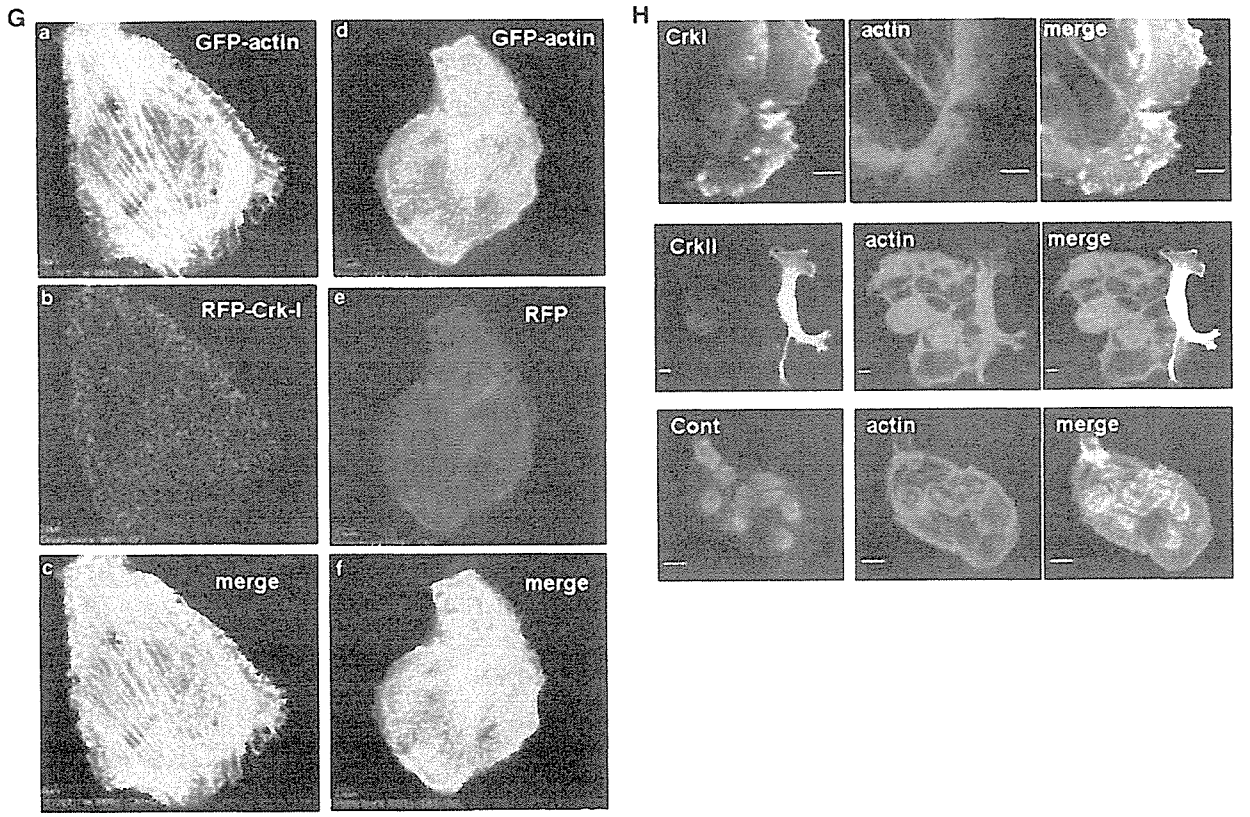

Figure 2 Continued.

clusters, and the thin cytoplasmic edge found in control MCAS cells was not observed in Crk knockdown cells in phase contrast microscopical analysis (Figure 2C). Actin staining demonstrated that dense actin bundles were present at the edge of the cytoplasm in Crk knockdown cells, and no lamellipodia was observed (Figure 2C). Immunofluorescence using antiphosphotyrosine and antipaxillin antibodies showed that the number of focal adhesions was significantly decreased in Crk knockdown cells (Figure 2D). Suppression of lamellipodia formation was confirmed by the transient transfection of the GFP fusion form of actin followed by time-lapse microscopy (Figure 2E and Supplementary data 1). Thirty-minute observations of single GFP-actin transfected cells showed that Crk knockdown cells can still move, even in the absence of lamellipodia (Figure 2E and Supplementary data 1 and 2). However, after 3 h of serum stimulation, cell scattering was much more prominent in control MCAS cells than in Crk knockdown cells (Figure 2F). To confirm the contribution of Crk to focal adhesion formation, we transiently transfected a expression plasmid for c-Crk-I fused to red fluorescent protein (RFP). Re-expression of c-Crk-I resulted in a recovery of the number of focal adhesions and also lamellipodia formation (Figure 2G and Supplementary data 3 and 4). It should be noted that in contrast to the RFP-Crk-I, we failed to transiently express RFP-Crk-II with unknown reason (data not shown). Thus, we re-expressed myc-tagged Crk-I or Crk-II in Crk knockdown MCAS cells, and found recovery of lamellipodia both by Crk-I and Crk-II (Figure 2H).

Analysis of Rac activity by pull-down assay and FRET-based time-lapse analysis

As Crk is known to regulate Rac through Dock180, we examined the activity of Rac. Consistent with the disappearance of lamellipodia, the amount of activated form of Rac was decreased in three Crk knockdown cells as determined by pull-down assay (Figure 3a). The decrease of Rac activity seemed to be correlated to the knockdown levels of Crk-II. To confirm the decrease of Rac activation, we utilized FRET-based time-lapse analysis for monitoring the activity of Rac (Itoh *et al*., 2002). Positive signals were observed after serum stimulation in control cells, but not in Crk knockdown cells (Figure 3b and Supplementary data 5 and 6).

Analysis of motility, invasion, adhesion and matrix production of Crk knockdown cells

To clarify the effect of Crk on cell motility, a phagokinetic track assay was performed. Significantly decreased motilities of Crk knockdown cells were observed in all three Crk knockdown MCAS cells (Figure 4a). Furthermore, Crk knockdown resulted in a marked suppression of cellular invasion as was deter-

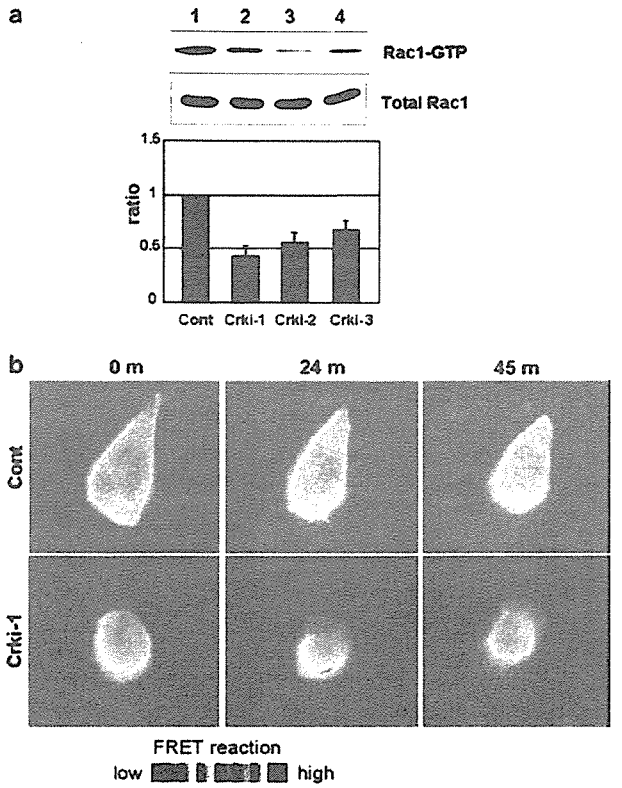

Figure 3 (**a**) Activity of Rac measured by pull-down assay in control and Crk knockdown cells. The GTP bound form of Rac was precipitated by GST-Pak-RBD and probed with anti-Rac Ab (upper panel). Total levels of Rac were visualized by immunoblotting using anti-Rac Ab (lower panel). Ratio of GTP-Rac and total level of Rac was quantified and described as bar graph with standard error. Lane 1, control; lane 2, Crki-1; lane 3, Crki-2; lane 4, Crki-3. (**b**) Time-lapse based FRET analysis of Rac activity in control (upper panels) and Crk knockdown Crki-1 (lower panels) cells 0, 24 and 45 min after 50 ng/ml of HGF stimulation. Reference of intensity was displayed at the bottom.

mined by a transwell assay (Figure 4b). As C3G was reported to regulate cell adhesion (Ohba *et al.*, 2001), an *in vitro* adhesion assay was performed. Only Crki-1 cells, not Crki-2 nor Crki-3, display a 15% reduction of adhesion on the laminin-coated culture dishes compared to control cells (Figure 4c). By pull-down assay, no significant alteration of Rap1 activity was observed in Crk knockdown MCAS cells (Figure 4d).

Anchorage-dependent and -independent growth of cells

As c-Crk has been shown to upregulate cell growth (Matsuda *et al.*, 1992a), we examined the role for Crk in growth of MCAS cells. Compared to parental cells and control cells, growth rates of three Crk knockdown cells were diminished when grown on non-coating culture plates (Figure 5a). We next examined the anchorage-independent growth of these cells by soft agar colony-forming assay. The numbers of medium sized colonies, 1.0–2.0 mm in diameter, were considerably decreased in all three of Crk knockdown cell lines (Figure 5b). Furthermore, large colonies, more than 2.0 mm in diameter, were detected in wild type and control cells, but not in Crk knockdown cells (Figure 5b). In contrast, the numbers of small sized colonies, 0.5–1.0 mm in size, were increased in Crk knockdown cells (Figure 5b).

Tumor formation assay in nude mice

Finally, we investigated the tumor-forming potential of Crk knockdown cells in nude mice. Three weeks after injection of cells, control MCAS cells formed tumors with $14 \times 10 \times 10\,mm^3$ in size and 0.8 g in weight on average. However, smaller sized tumors, with mean volumes of $10 \times 6 \times 5\,mm^3$ and mean weight of 0.4 g, were observed following injection with Crk knockdown cells (Table 1 and Figure 6a). Histopathological analysis demonstrated that control cells formed tumors with necrosis both in center and peripheral area of the tumor nodules (Table 1 and Figure 6b and c). Tumors formed by Crk knockdown cells exhibited central necrosis, but no small necrotic focus was observed in the peripheral area of the tumor (Figure 6b and c). Although the MCAS cell line was established from a surgical specimen of mucinous adenocarcinoma, the tumors formed in nude mice did not exhibit prominent mucous secretion. In contrast, in tumors formed by Crk knockdown cells, tubular formation was remarkable and significant mucous production was demonstrated by both of hematoxylin and eosin (H&E) and periodic acid Schiff (PAS) staining (Figure 6d).

We also injected established cell lines in the peritoneal cavity of nude mice and examined the potential of tumor growth as peritonitis carcinomatosa, which is one of the characteristic features of human ovarian cancer. Autopsy demonstrated that small nodules, 1.0–5.0 mm in size, were disseminated in the peritoneal cavity of mice injected with control cells (Table 1). Microscopically, tumor cells had invaded into the retroperitoneum with remarkable lymphatic vessel infiltration of the peritoneal wall (Figure 6e). In contrast, there was no evidence of tumor growth in mice injected with Crk knockdown cells (Figure 6e).

Discussion

Despite recent advancements in cancer therapy, aggressive tumors, characterized by invasion and metastasis, are still associated with poor prognosis. Among the most highly invasive human cancers, ovarian cancer, especially mucinous adenocarcinoma, is distinguishable due to its frequent intraperitoneal dissemination as well as local invasion. To control the dissemination of tumor cells, an understanding of the physiological mechanism of cell movement is important. ECM stimuli-provoked signals are transmitted, by way of cellular surface receptors such as integrins, to downstream effectors such as the Rho family of small GTPases, which play a central role in cell motility. However, regulation of the activity of small GTPases is complex and is still under investigation.

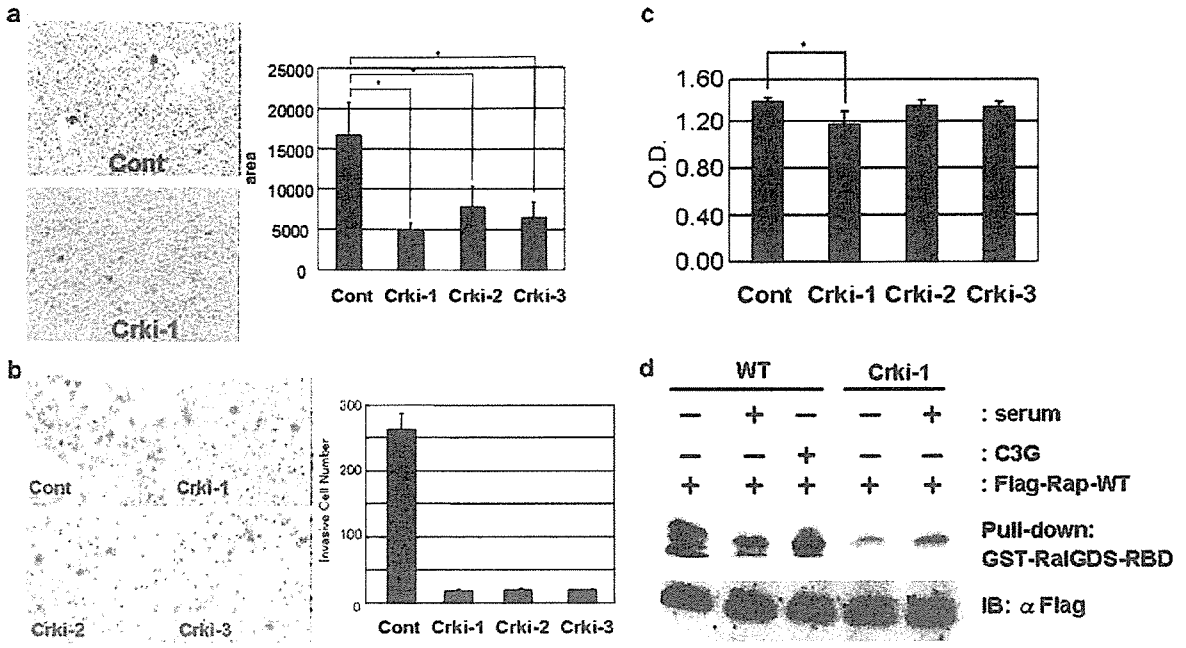

Figure 4 (**a**) Analysis of cell motility of control MCAS cells and Crk knockdown cells by phagocytotic track assay. Phase-contrast microscopic observation (left panels) of the moved area. Moved areas were measured and described as bar graphs (right). The difference among groups was analysed statistically by ANOVA, $F=82.9$, $P<0.01$. (**b**) Invasion of MCAS cells were analysed by transwell assay. The number of moved cells were counted and described as bar graph with standard error. (**c**) Cell adhesion was analysed on laminin-coated dishes and described as bar graph, $F=11.75$, $P<0.01$ in Crki-1 cells. No significance was found between control and Crki-2 and -3 cells. (**d**) Measurement of Rap activity. Wild type and Crki-1 cells were transfected with Flag-Rap1 expression plasmids and with or without serum stimulation for 30 min cells were lysed and GTP-Rap1 was precipitated by GST-RalGDS-RBD, and probed with anti-Flag tag Ab (upper panel). pCAGGAS-C3G was transfected as positive control for the assay. Total levels of exogenous Rap-1 were demonstrated by using anti-Flag tag Ab (lower panel).

Recently, we and others reported that signaling adaptor protein Crk is overexpressed in human cancers (Nishihara *et al*., 2002c; Miller *et al*., 2003; Takino *et al*., 2003). Because Crk links the components of focal adhesion and GEFs for small GTPases, including Rho family proteins, overexpression of Crk may be one of the key events leading to the deterioration of cell motility. To define the precise role for Crk in malignancy of human cancers, we employed siRNA to knock down Crk expression in the human ovarian mucinous adenocarcinoma cell line MCAS. When Crk expression was diminished, cells did not form lamellipodia, probably because of the loss of focal adhesion formation as was shown by immunofluorescence study using antipaxillin and antiphosphotyrosine antibodies. Time-lapse analysis for GFP-actin transfected MCAS cells clearly confirmed that Crk knockdown decreased lamellipodia formation. In Crk knockdown cells, Rac activity was decreased and the motility and invasion potentials were also disturbed. These data suggest that Crk bound to Dock180, which is a GEF for Rac, may play a role in the regulation of motility in MCAS cells.

We did not observe compensatory overexpression of CrkL in CrkII knockdown mince (Figure 2a). By using retroviral insertional mutation technique, CrkII depleted mice were established. In these mice, the protein expression level of CrkI was intact. The authors of this paper did not examine the levels of CrkL (Imaizumi *et al*., 1999). Furthermore, in CrkL knockout study, it is described that the expression level of CrkII was not altered in the mice lacking CrkL (Hemmeryckx *et al*., 2002). In fact, we have established CrkII knockdown cells by using three human sarcoma cell lines and a glioblastoma cell line, and we did not observe the increase of the levels of CrkL in these cell lines (data not shown).

In general, the major components of focal adhesions have been shown to include talin, vinculin, tensin, paxillin and $p130^{Cas}$. Considering the decrease of the number of focal adhesions in Crk knockdown cells, Crk may be one of the essential components of a certain fraction of focal adhesion complexes. Because the focal adhesions still presented at the border of the cytoplasm in Crk knockdown cells, Crk may not be required to maintain the focal adhesions, at least, located at the cytoplasmic edge.

As C3G and Rap1 have been shown to regulate cell adhesion, we analysed the alteration of cell attachment to several ECMs including fibronectin, collagen, laminin and hyarulonic acid. Although, only Crki-1 cells exhibit small reduction of attachment to laminin (Figure 4c), basically, no significant suppression of attachment for ECMs was observed in Crk knockdown cells. Correlating to these results, Rap-1 activity was also not changed in Crk knockdown MCAS cells, although serum stimulation did not function as positive control for the

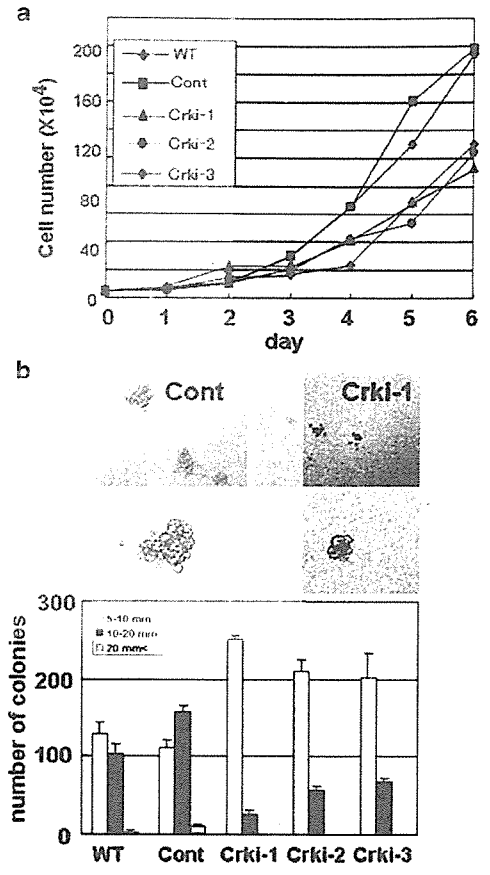

Figure 5 (**a**) Growth rates of control and three Crk knockdown cells were measured for 6 days on plastic plates. (**b**) Colony formation assay. Upper panels showed the formed colonies in soft agar. Numbers of colonies were measured and displayed as bar graph. Open bar, colonies sized 5–10 mm in diameter. Closed bar, colonies 10–20 mm in diameter and gray bar, more than 20 mm in diameter.

Table 1 Tumor formation in nude mice

	Control	*Crki-1*	*Crki-2*
s.c.[a] *(injected number n = 5)*			
Number	5	5	5
Size (mm)	14 × 11 × 10	10 × 6 × 5	10 × 7 × 5
Weight (g)	0.8	0.4	0.4
I.P.[b] *(injected number n = 5)*			
Number	3	0	2
Dissemination	Yes	No	No[c]

[a]s.c., subcutaneous injection. [b]i.p., intraperitoneal injection. [c]Single small nodule 2 mm in size presented.

assay (Figure 4d). Therefore, at least in MCAS cells, Crk/C3G-dependent Rap activation may not be a major mechanism of control of cell adhesion to ECMs. The reason why the effect of Crk/C3G/Rap1-dependent signaling was not dominantly observed in MCAS cells should be examined in future.

We also analysed the effect of Crk on the growth of MCAS cells, and found that growth rates of Crk knockdown cells were considerably lower than those of control cells. Thus, Crk may control the cell cycle through a C3G/R-Ras/Jun kinase-dependent mechanism, in addition to activating Ras/Erk through Sos (Tanaka *et al*., 1997; Tanaka and Hanafusa, 1998). Furthermore, the suppression of anchorage-dependent growth of Crk knockdown cells seems to be reasonable because both cell motility and proliferation were down-regulated in these cells. Subcutaneous injection of the cells into nude mice supported the *in vitro* observations suggesting that Crk may play a role in tumor cell growth and invasion. We confirmed that Crk knockdown cells did not exhibit apoptotic phenotype by using TUNEL stain and FACS analysis for cell cycle. It should be noted that Crk-I was clearly diminished in all three Crk knockdown cells, but Crk-II remained at diefferential levels. The decrease of Rac-activity in three Crk knockdown cells seemed to be related to the levels of remained Crk-II. However, there was no significant difference in the suppression of anchorage-dependent and independent growth of three Crk knockdown cells. It should be noted that we have established several Crk knockdown cells by using human sarcoma and brain tumor cell lines in which Crk-II remained differentially. But in all of the Crk knockdown cell lines, significant decrease of cell growth was observed (T Watanabe, L Wang and S Tanaka, in preparation).

Histopathological analysis showed that reduction of Crk expression enhanced the mucous production of cells. In culture, Crk knockdown cells exhibited matrix production as was demonstrated by the particle exclusion assay. Cells stained positive for PAS, implying that such matrix contains mucin, which may be indicative of cell differentiation. Together with the report that Crk has been shown to be overexpressed in tumor cells with poor prognosis (Miller *et al*., 2003), these results suggested that eliminated Crk expression may induce differentiation in tumor cells.

Intraperitoneal injection of tumor cells resulted in a remarkable difference in tumor formation between control and Crk knockdown cells. Crk knockdown cells did not form any tumors in the peritoneal cavity, while control cells produced tumor nodules with lymphoid vessel infiltration. From these results, the attenuation of cell motility, invasion or adhesion may be critical in the survival and growth of tumor cells in the peritoneal cavity. Alternatively, the production of matrix metalloproteinases (MMPs) may be involved in the tumor forming ability in the peritoneal cavity, because Crk was shown to regulate MMP production in rat fibroblasts 3Y1 cells (Liu *et al*., 2000).

The results of this study suggest that Crk may be critical for the malignant potential of MCAS cells, presumably by enhancing tumor cell motility, invasion and dissemination. Therefore, the development of a chemical compound that specifically inhibits the association of SH2 or SH3 domains of Crk to their targets may have therapeutic value in future.

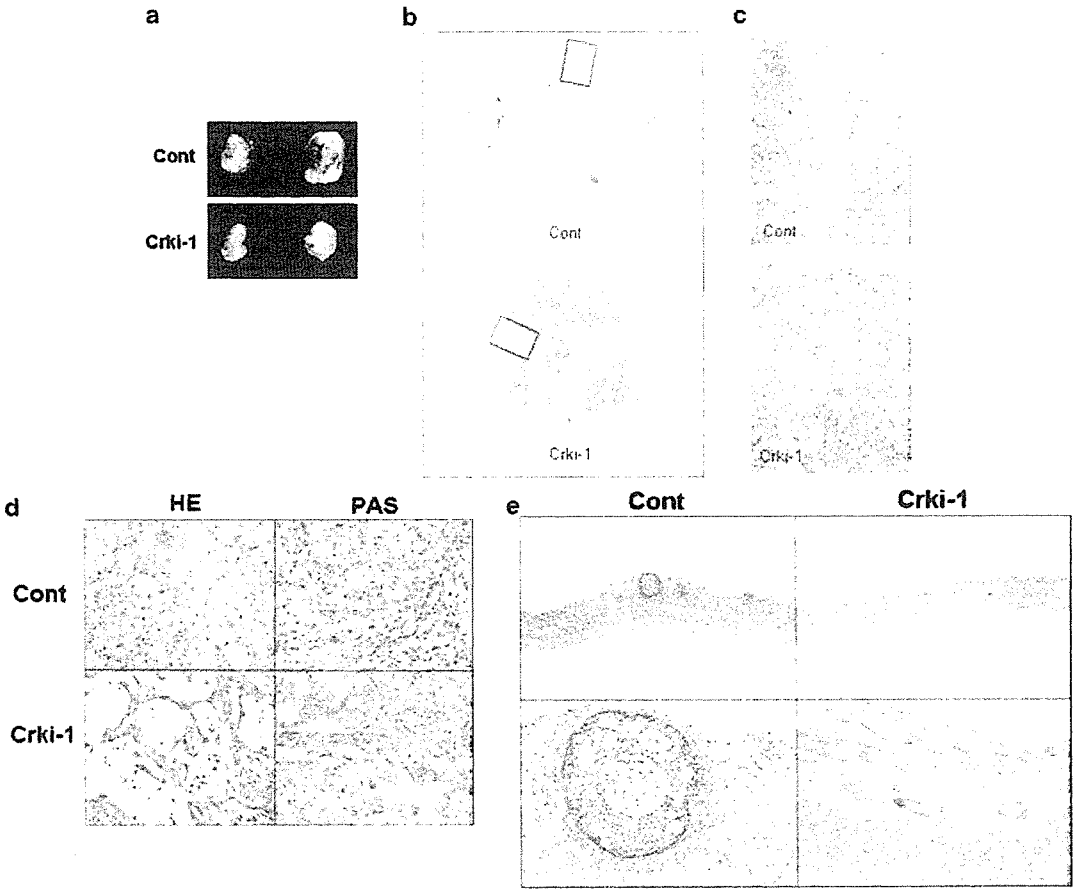

Figure 6 (a) Tumor formation of control (Cont) or Crk knockdown (Crki) MCAS cells at the back of nude mice. Macroscopic observation of surgically resected tumor nodules. (b) Histopathological analysis of resected tumors. H&E stain. (c) Histopathological analysis of peripheral region of each tumor. (d) Higher magnification of tumors. H&E and PAS stainings. (e) Analysis of the peritoneal cavity of MCAS-injected mice. Histopathological examination of peritoneal walls with H&E stain (upper panels). Lower panels showed the lymphoid vessel of the peritoneal walls.

Materials and methods

Cell lines and antibodies

MCAS, a human mucinous cystadenocarcinoma cell line (JCRB0240), was purchased from Health Science Research Resources Bank (HSRRB, Osaka, Japan) and maintained in Dulbecco's modified minimal essential medium (DMEM) supplemented with 10% fetal bovine serum (FBS), 2 mM L-glutamine, and 100 U/ml penicillin and streptomycin. The recombinant antibody (Ab) for phosphotyrosine (RC20H), mouse monoclonal antibody (mAb) for Crk (clone 22) and rabbit polyclonal Abs for p130^{Cas} (C20) and paxillin, were purchased from Transduction Laboratories (Lexington, KY, USA). Antibodies for C3G (C19), CrkL (C20), and Dock180 (H4) were obtained from Santa Cruz Biotechnology (Santa Cruz, CA, USA).

Plasmids

The plasmid used for Crk interference, pSUPER (suppression of endogenous RNA)-Crk-interference (pSUPER-iCrk) with sequence of 5′-UGCCUACGACAAGACAGCC-3′ corresponding to 746–765 bp of human c-Crk-II gene, was described previously (Nagashima *et al.*, 2002). pCXN2-Flag-Crk and pCXN2-Flag-CrkL were generated in our laboratory. pGEX-Crk-I, pGEX-Crk-II, pGEX-Crk-SH3(N) and pGEX-CRK-SH3(C) were described previously (Tanaka *et al.*, 1993). pGEX-PAK2-RBD was also described previously (Nishihara *et al.*, 2002b).

Immunoprecipitation and immunoblotting

Cells were lysed with lysis buffer containing 150 mM NaCl, 10 mM Tris hydrochloride (pH 7.5), 5 mM EDTA, 10% glycerol, 0.5% Nonidet P-40, 1 mM sodium orthovanadate, 1 mM phenylmethylsulfonyl fluoride (PMSF), 50 mM sodium fluoride. Lysates were incubated with antibodies for 1 h at 4°C, followed by incubation with protein G- or protein A-sepharose beads (Calbiochem, Darmstadt, Germany) for 1 h at 4°C while rotating. Immunoprecipitates were separated by sodium dodecyl sulfate–polyacrylamide gel electrophoresis and immunoblotted onto PVDF (polyvinylidene fluoride) filter (Immobilon, Millipore Co., Bedford, MA, USA). The filter was blocked with 3% bovine serum albumin and then incubated with primary Abs followed by peroxidase-conjugated secondary Abs. Positive signals were detected by enhanced chemiluminescence system (Amersham Biosciences,

Piscataway, NJ, USA) and analysed by LAS-1000 detection system (Fuji Film, Tokyo, Japan).

Establishment of Crk knockdown MCAS cells
Cells were co-transfected with 3 μg of pSUPER-iCrk and 0.6. μg of pBabe-puro plasmid, followed by selection with 2 μg/ml puromycin containing medium for 2–3 weeks. Colonies were isolated and the expression levels of Crk were analysed by immunoblotting.

Immunofluorescence analysis of the cells
Subconfluent cells grown on glass coverslips were fixed with 3.7% formaldehyde in phosphate-buffered saline (PBS) for 15 min and permeabilized with 0.2% Triton X-100 in PBS for 5 min. To visualize actin filaments (F-actin), cells were stained with TRITC-conjugated phalloidine (1 μg/ml) for 30 min and observed under a confocal immunofluorescence microscope (Olympus, Japan). For time-lapse imaging, MCAS cells were transfected with the mammalian expression plasmid pEGFP-actin, 36 h later cells were replated onto glass dishes and GFP signal was obtained every 90 min using a time-lapse system (Nippon Roper, Chiba, Japan). Images were analysed using Metamorph software (Molecular Probe, USA).

GST pull-down assay for detection of Crk-binding proteins
Cell lysates containing 300 μg of protein were incubated with 20 μg of either GST, GST-CrkI, GST-CrkII, GST-Crk-SH2 or GST-Crk-SH3(N) for 1 h at 4°C, followed by incubation with glutathione-sepharose beads (Amersham Bioscience, Piscataway, NJ, USA) for 1 h at 4°C while rotating. Proteins bound to the beads were analysed by immunoblotting.

Pull-down assay for Rac1 activity
Detection of the GTP-bound form of Rac1 was performed as described previously (Nishihara *et al*., 2002a). Cells were lysed with buffer containing 25 mM HEPES (pH 7.4), 150 mM NaCl, 10% glycerol, 1 mM EDTA, 1% NP40, 10 mM $MgCl_2$, 1 μg/ml aprotinin and 1 mM PMSF. Lysates were centrifuged at 12 000 r.p.m. at 4°C for 1 min, and the supernatants were incubated with 10 μg of purified GST-PAK2-RBD and glutathione-Sepharose 4B beads. The resulting precipitants were analysed by immunoblotting with anti-Rac1.

FRET-based analysis of Rac activity
pRachu-Rac-CAAX was transfected into MCAS cells, and 30 h later cells were cultured in DMEM with 2% FBS for 8 h. After 10% FBS stimulation, FRET-based analysis of Rac activity was performed following the methods established by Dr M Matsuda (Osaka University, Japan) (Itoh *et al*., 2002).

Phagokinetic track assay
To analyse cell motility, 2×10^3 cells in DMEM were spread on 24×24 mm^2 coverslips precoated with 1% BSA and colloidal gold particles. After incubating for 24 h, cells were fixed with 3.5% formaldehyde, and the phagokinetic range for each cell was measured using Image Gauge software (Fuji Film, Tokyo, Japan).

Adhesion assay
For analysis of adhesion, 4×10^4 cells were suspended in 0.1 ml of DMEM, plated on 96-well plates, and incubated for 1 h at 37°C. The bound cells in each well were lysed, stained with 0.1% crystal violet, and quantified by spectrophotometer at OD A590 nm.

Invasion assay
The lower surface of the filter Bio Coat Matrigel Invasion Chamber (BD Biosciences, Franklin Lakes, NJ, USA) was coated with 1 μg of collagen. Fifty thousands cells were seeded in the upper chambers (24-well chambers) in 0.5 ml of serum-free medium containing 0.01% BSA and 3.3 mM glucose, and the bottom chambers contained the appropriate medium with 1% FBS as a chemo-attractant. The non-invading cells on the upper surface of the filters were removed by wiping with a cotton swab. Cells at the bottom side of the membranes were fixed with ethanol, and stained with 0.5% methyl blue. The number of cells invading through the matrigel membrane was counted in microscopic fields at $\times 200$ magnification. To minimize the bias, at least three randomly selected fields were counted. Data were averages of triplicate determinants for each condition.

Measurement of growth rates
To measure growth rates, 1×10^5 cells were seeded onto 60-mm diameter plates with DMEM containing 10% FBS, and the numbers of cells were counted everyday using a hemocytometer (Fisher Scientific).

Colony formation assay
To analyse the anchorage-independent growth of cells, 1×10^4 of cells were plated in 60-mm diameter plates with 3 ml of 0.4% noble agar in DMEM in 10% FBS, overlaying 5 ml of 0.5% bacto agar in DMEM with 10% FBS. Colonies were scored 3 weeks after plating. The number of colonies larger than 5 mm in diameter was counted under a microscope.

In vivo *tumor formation assay in nude mice*
MCAS-Crki1 cell line, in which the expression levels of both c-Crk-I and c-Crk-II was most efficiently suppressed among three established clones (Figure 2a), were injected into mice. Subcutaneously or intraperitoneally, 1×10^6 cells were injected into three of the 6-week-old female nude mice, BALB/cA Jcl-nu (nu/nu) (CLEA Japan Inc., Japan). The mice were euthanized 21–24 days after injection, and tumors were removed and weighed. A histopathological examination was performed, including hematoxylin and eosin stain and periodic acid Schiff stain.

Acknowledgements

We thank Dr Michiyuki Matsuda (Osaka University, Japan) for setting up a FRET-based time-lapse microscopy and the providing plasmids for monitoring the activity of small GTPases in a single cell. This study was supported in part by the Japan–China Sasakawa Medical Fellowship, by Grants-in-Aid from the Ministry of Education, Science, Culture, and Sports, and of the Ministry of Health, Labor, and Welfare.

References

Albert ML, Kim J-I, Birge RB. (2000). *Nat Cell Biol* **2**: 899–905.

Brugge JS. (1998). *Nat Genet* **19**: 309–311.

Brugnera E, Haney L, Grimsley C, Lu M, Walk SF, Tosello-Trampont AC *et al*. (2002). *Nat Cell Biol* **4**: 574–582.

Chen Z, Fadiel A, Feng Y, Ohtani K, Rutherford T, Naftolin F. (2001). *Cancer* **92**: 3068–3075.
Feller SM. (2001). *Oncogene* **20**: 6348–6371.
Gotoh T, Hattori S, Nakamura S, Kitayama H, Noda M, Takai Y *et al.* (1995). *Mol Cell Biol* **15**: 6746–6753.
Gumbiner BM. (1996). *Cell* **84**: 345–357.
Gumienny TL, Brugnera E, Tosello-Trampont AC, Kinchen JM, Haney LB, Nishiwaki K *et al.* (2001). *Cell* **107**: 27–41.
Hall A. (1998). *Science* **279**: 509–514.
Hasegawa H, Kiyokawa E, Tanaka S, Nagashima K, Gotoh N, Shibuya M *et al.* (1996). *Mol Cell Biol* **16**: 1770–1776.
Hemmeryckx B, Reichert A, Watanabe M, Kaartinen V, de Jong R, Pattengale PK *et al.* (2002). *Oncogene* **21**: 3225–3231.
Imaizumi T, Araki K, Miura K, Araki M, Suzuki M, Terasaki H *et al.* (1999). *Biochem Biophys Res Commun* **266**: 569–574.
Itoh RE, Kurokawa K, Ohba Y, Yoshizaki H, Mochizuki N, Matsuda M. (2002). *Mol Cell Biol* **22**: 6582–6591.
Iwahara T, Akagi T, Shishido T, Hanafusa H. (2003). *Oncogene* **22**: 5946–5957.
Judson PL, He X, Cance WG, Van Le L. (1999). *Cancer* **86**: 1551–1556.
Kiyokawa E, Hashimoto Y, Kobayashi S, Sugimura H, Kurata T, Matsuda M. (1998). *Genes Dev* **12**: 3331–3336.
Lauffenburger DA, Horwitz AF. (1996). *Cell* **84**: 359–369.
Liu E, Thant AA, Kikkawa F, Kurata H, Tanaka S, Nawa A *et al.* (2000). *Cancer Res* **60**: 2361–2364.
Matsuda M, Reichman CT, Hanafusa H. (1992a). *J Virol* **66**: 115–121.
Matsuda M, Tanaka S, Nagata S, Kojima A, Kurata T, Shibuya M. (1992b). *Mol Cell Biol* **12**: 3482–3489.
Mayer BJ, Hamaguchi M, Hanafusa H. (1988). *Nature* **332**: 272–275.
Miller CT, Chen G, Gharib TG, Wang H, Thomas DG, Misek DE *et al.* (2003). *Oncogene* **22**: 7950–7957.
Mochizuki N, Ohba Y, Kobayashi S, Otsuka N, Graybiel AM, Tanaka S *et al.* (2000). *J Biol Chem* **275**: 12667–12671.
Nagashima K, Endo A, Ogita H, Kawana A, Yamagishi A, Kitabatake A *et al.* (2002). *Mol Biol Cell* **13**: 4231–4242.
Nishihara H, Maeda M, Oda A, Tsuda M, Sawa H, Nagashima K *et al.* (2002a). *Blood* **100**: 3968–3974.
Nishihara H, Maeda M, Tsuda M, Makino Y, Sawa H, Nagashima K *et al.* (2002b). *Biochem Biophys Res Commun* **296**: 716–720.
Nishihara H, Tanaka S, Tsuda M, Oikawa S, Maeda M, Shimizu M *et al.* (2002c). *Cancer Lett* **180**: 55–61.
Ohba Y, Ikuta K, Ogura A, Matsuda J, Mochizuki N, Nagashima K *et al.* (2001). *EMBO J* **20**: 3333–3341.
O'Neill GM, Fashena SJ, Golemis EA. (2000). *Trends Cell Biol* **10**: 111–119.
Sheetz MP, Felsenfeld DP, Galbraith CG. (1998). *Trends Cell Biol* **8**: 51–54.
Summy JM, Gallick GE. (2003). *Cancer Metastasis Rev* **22**: 337–358.
Takino T, Nakada M, Miyamori H, Yamashita J, Yamada KM, Sato H. (2003). *Cancer Res* **63**: 2335–2337.
Tanaka S, Hanafusa H. (1998). *J Biol Chem* **273**: 1281–1284.
Tanaka S, Hattori S, Kurata T, Nagashima K, Fukui Y, Nakamura S *et al.* (1993). *Mol Cell Biol* **13**: 4409–4415.
Tanaka S, Morishita T, Hashimoto Y, Hattori S, Nakamura S, Shibuya M *et al.* (1994). *Proc Natl Acad Sci USA* **91**: 3443–3447.
Tanaka S, Ouchi T, Hanafusa H. (1997). *Proc Natl Acad Sci USA* **94**: 2356–2361.
Tsuda M, Tanaka S, Sawa H, Hanafusa H, Nagashima K. (2002). *Cell Growth Differ* **13**: 131–139.
Yano H, Uchida H, Iwasaki T, Mukai M, Akedo H, Nakamura K *et al.* (2000). *Proc Natl Acad Sci USA* **97**: 9076–9081.

Supplementary Information accompanies the paper on Oncogene website (http://www.nature.com/onc)

Journal of Biochemistry and Molecular Biology, Vol. 39, No. 2, March 2006, pp. 132-139

JOURNAL OF Biochemistry and Molecular Biology

Review

Vascular Endothelial Cadherin-mediated Cell-cell Adhesion Regulated by a Small GTPase, Rap1

Shigetomo Fukuhra, Atsuko Sakurai, Akiko Yamagishi, Keisuke Sako and Naoki Mochizuki*
Department of Structural Analysis, National Cardiovascular Center Research Institute, 5-7-1 Fujishirodai, Suita, Osaka 565-8565, Japan

Received 28 February 2006

Vascular endothelial cadherin (VE-cadherin), which belongs to the classical cadherin family, is localized at adherens junctions exclusively in vascular endothelial cells. Biochemical and biomechanical cues regulate the VE-cadherin adhesive potential by triggering the intracellular signals. VE-cadherin-mediated cell adhesion is required for cell survival and endothelial cell deadhesion is required for vascular development. It is therefore crucial to understand how VE-cadherin-based cell adhesion is controlled. This review summarizes the inter-endothelial cell adhesions and introduces our recent advance in Rap1-regulated VE-cadherin adhesion. A further analysis of the VE-cadherin recycling system will aid the understanding of cell adhesion/deadhesion mechanisms mediated by VE-cadherin in response to extracellular stimuli during development and angiogenesis.

Keywords: Adherens junction, Permeability, Rap1, Vascular endothelial-cadherin (VE-cadherin)

Introduction

Vascular endothelial cells aid in the regulation of blood flow for the supply of nutrients to the tissues. Morphologically, vascular endothelial cells make cell-to-cell contact, not only with the neighboring endothelial cells, but also with supporting pericytes in the capillaries. In addition, they are supported by the extracellular matrix and inner basal lamina (Davis and Senger, 2005). Vascular endothelial cell-cell adhesions are organized mainly by adherens junctions (AJs), tight junctions (TJs), and gap junctions (GJs) as other epithelial cell-cell adhesions (Fig. 1). The most striking difference between endothelial cell-cell contacts and epithelial cell-cell contacts is that the junctions are intermingled in the former while TJ-AJ-GJ is organized from the apical to base side in the latter. To date, the function of specific AJ-, TJ-, and GJ-constituting molecules within endothelial cells have extensively analyzed. It is essential for endothelial cells to maintain cell-cell adhesion in order to keep morphological integrity and quiescence.

The extracellular stimuli loosen cell-cell contacts prior to promoting proliferation of vascular endothelial cells. Such includes vascular endothelial growth factor (VEGF) and its related factors (reviewed in (Yancopoulos *et al.*, 2000) and (Gale and Yancopoulos, 1999)). VEGF was initially described as a vascular permeability factor, as its name indicates (Keck *et al.*, 1989). On the contrary, Angiopoietin (Ang) stabilizes the cell-cell contacts and reduces vascular permeability via activation of the Tie2 receptor tyrosine kinase. Both VEGF-VEGF receptor (VEGF-R), and Ang-Tie2 signaling are required for embryonic vascular development (Shalaby *et al.*, 1995; Fong *et al.*, 1995; Suri *et al.*, 1996; Gale *et al.*, 2002). Another receptor tyrosine kinase system, ephrin-Eph tyrosine kinase, is also indispensable for vascular development. Ephrin is anchored by GPI (ephrin-A family), or single spanning (ephrin-B family), and therefore cell-cell contacts can trigger Eph receptor activation, resulting in either a repulsive or adhesive action between vascular endothelial cells. Thus, ephrin-Eph is believed to induce the motility of vascular endothelial cells and to determine the lineage of arterial endothelial cells and venous endothelial cells (Adams and Klein, 2000; Nagashima *et al.*, 2002).

In this review, we highlight the recent progress in studies concerning the adhesion molecules of AJ and TJ in vascular endothelial cells, particularly vascular endothelial cadherin (VE-cadherin)-based AJ formation. In addition, we present our recent findings, which suggest that the balance between VE-cadherin trafficking and the stabilization of assembled VE-cadherin regulates the integrity of the endothelial cells. We further suggest the importance of the trafficking regulated by extracellular stimuli, although recent studies have illuminated the mechanism of assembly and disassembly of adhesion molecules.

*To whom correspondence should be addressed.
Tel: 81-6-6833-5012 ext 2508; Fax: 81-6-6835-5461
E-mail: nmochizu@ri.ncvc.go.jp

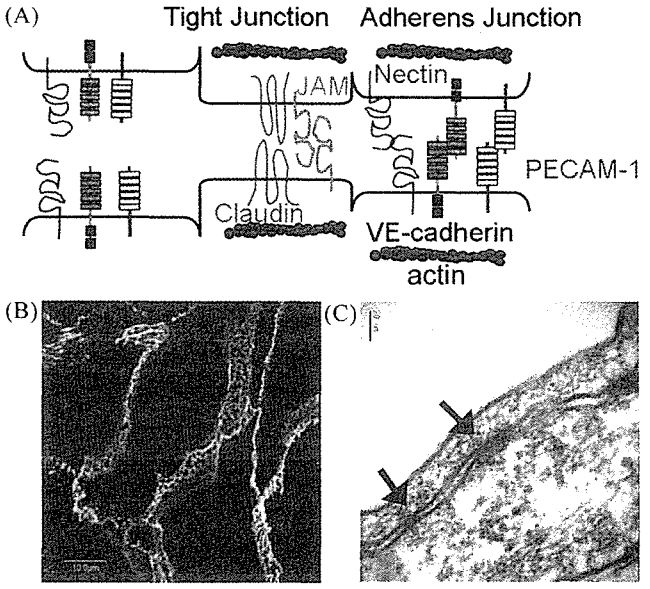

Fig. 1. Structural characteristic of endothelial cell junctions. (A) Vascular endothelial junction molecules. VE-cadherin, Nectin, and PECAM-1 are localized at the adherens junction, whereas JAM and Claudin are at the tight junction. (B) Cultured human umbirical vein endothelial cells (HUVECs) are immunostained with anti-VE-cadherin antibody and visualized by fluorescence (green)-conjugated secondary antibody. Note that VE-cadherin are found belt-shaped on the overlapped peripheral membrane of endothelial cells, suggesting that AJs and TJs are intermingled. (C) Electron microscope image of overlapped endothelial cells. Arrows denote the adherens junctions.

Junctional molecules of vascular endothelial cells

AJs consist of VE-cadherin (Lampugnani *et al.*, 1995), Nectin-2 (Reymond *et al.*, 2004), and platelet and endothelial cell adhesion molecule-1 (PECAM-1) (Fig. 1) reviewed in (Dejana, 2004). VE-cadherin belongs to the classical cadherin superfamily and exhibits cis and trans homophilic association via external 5 cadherin domains in a Ca^{2+}-depedent manner (Chappuis-Flament *et al.*, 2001). It spans the plasma membrane and binds to p120catenin (p120ctn) and β-catenin (β-ctn) in the proximal and distal cytoplasmic domain, respectively. Because β-ctn directly associates with α-ctn, which is connected to cortical actin, VE-cadhrerin is supported by cytoskeletal actin. However, this scheme has been recently questioned by two groups (Yamada *et al.*, 2005; Drees *et al.*, 2005). These two groups suggest a more dynamic role of α-ctn in cortical actin assembly near the cadherin-based adhesion. Likewise, nectin is linked to cortical actin fibers by binding to afadin, which is associated with actin fibers. PECAM-1 is also reported to be associated with β-ctn. Thus, VE-cadherin, nectin, and PECAM-1 may be lined by cortical action filaments. Other cadherin family members, N-cadherin and VE-cadherin2 are reported to be expressed in vascular endothelial cells (Salomon *et al.*, 1992; Telo' *et al.*, 1998). It is not yet confirmed whether N-cadherin is localized to the inter-endothelial cell-cell contacts (Salomon *et al.*, 1992; Navarro *et al.*, 1998; Luo and Radice, 2005). Although VE-cadherin2 is a single transmembrane protein like VE-cadherin and N-cadherin, it does not contain catenin-binding sites in the cytoplasmic domain. VE-cadhrin2-deficient mice do not exhibit gross vascular developmental abnormality. Thus, the function of VE-cadherin2 remains to be analyzed.

Nectins and cadherins cooperatively function for the formation of AJ. However, there is a striking difference between nectins and cadherins upon homophilic association. Cadherin, but not nectin, requires Ca^{2+} for their homophilic association. The research team of Takai demonstrated that the c-Src-Crk-C3G-Rap1 signaling, triggered by nectin engagement upon cell-cell contact, is important for AJ formation (Fukuyama *et al.*, 2005). Furthermore, they demonstrated that activated Rap1-afadin complex binds to p120ctn, thereby regulating cadherin-based AJ formation. Molecular regulation of the nectin family molecules has been extensively studied and reviewed by Takai's group (Takai and Nakanishi, 2003; Sakisaka and Takai, 2004).

PECAM-1 has six external immunoglobulin-like domains, a single transmembrane domain, and a cytoplasmic domain (Newman and Newman, 2003). The cytoplasmic domain has an ITIM motif that provides a binding site for SHP2 (Jackson *et al.*, 1997; Masuda *et al.*, 1997). Like that of other cell-cell adhesion molecules, PECAM-1-to- PECAM-1 bonding is achieved through homophilic trans-interaction. Therefore, PECAM-1 engagement is thought to provoke intracellular signaling via adaptor/docking molecules including SHP2, SHP1, PLCg, and Grb2 (reviewed in Newman and Newman, 2003). Interestingly, PECAM-1 may be involved in the mechanotransduction pathway together with VE-cadherin (Osawa *et al.*, 2002; Newman and Newman, 2003).

TJs are made up of junctional adhesion molecule (JAM) family members, endothelial cell-selective adhesion molecules (ESAM), occuludin, claudin (1, 5, and 12) and nectin (reviewed in (Dejana, 2004)). Interestingly, nectin is localized to within AJs and TJs. JAM, ESAM, claudin, and occudin are associated with zona occludens-1 (ZO1) (Gumbiner *et al.*, 1991; Wong and Gumbiner, 1997; Tsukita *et al.*, 2001; Bazzoni, 2003). Because ZO1 binds to filamentous actin, these TJ molecules are linked to the actin cytoskeleton. Other PDZ domain-containing molecules, such as MAGUK with an inverted domain structure-1 (MAGI-1) and ZO2, are capable of associating with the intracellular C-terminal region of JAM family members (Shoji *et al.*, 2000; Laura *et al.*, 2002; Wegmann *et al.*, 2004).

Signaling mediated by VE-cadherin and signaling triggered by VE-cadherin engagement

Vascular endothelial cells receive biochemical signals as well as biomechanical signals (Shay-Salit *et al.*, 2002). VE-

cadherin regulates β-ctn as a transcription factor. Because the cytoplasmic domain binds β-ctn, which translocates into the nucleus where it associates with Tcf and activates transcription of multiple genes, the association of β-ctn and VE-cadherin inhibits β-ctn-mediated transcriptional activation (Caveda *et al.*, 1996).

The tyrosine residues of cytoplasmic domain of VE-cadherin are phosphorylated by Src family kinases upon tumor necrosis factor stimulation (Nwariaku *et al.*, 2004; Lambeng *et al.*, 2005). Furthermore, extravasation of blood cells induces VE-cadherin phophorylation. Subsequently, tyrosine-phosphorylated VE-cadherin provides the docking sites for multiple signaling molecules including SHP2, phosphatidylinositol 3'-kinase (PI3K) and Shc(Ukropec *et al.*, 2000; Zanetti *et al.*, 2002; Hudry-Clergeon *et al.*, 2005). In contrast, phosphorylated VE-cadherin does not bind to p120ctn and β-ctn (Potter *et al.*, 2005). Thus, phosphorylation and dephosphorylation of VE-cadherin is implicated in intracellular signaling and stabilization of cell-cell contacts.

VEGF-VEGF-R signaling regulates permeability, vascular endothelial cell proliferation, and cell survival. VE-cadherin is involved in VEGF-mediated cell signaling (Esser *et al.*, 1998; Zanetti *et al.*, 2002; Grazia *et al.*, 2003a). VE-cadherin associates with VEGF-R2 and modulates the VEGF-R2-mediated signaling (Carmeliet *et al.*, 1999; Rahimi and Kazlauskas, 1999; Weis *et al.*, 2004). VE-cadherin further involves the phosphatase DEP-1 for cell-cell contact-dependent inhibition of cell-proliferation induced by VEGF (Grazia *et al.*, 2003b). This previous line of evidence indicates that VE-cadherin is required for VEGF-R2-mediated signals at cell-cell contacts.

Classical cadherin ligation induces the activation of Rho family GTPases (Fukata and Kaibuchi, 2001; Wheelock and Johnson, 2003). VE-cadherin homophilic ligation activates Rac1 and Cdc42 (Kovacs *et al.*, 2002; Kouklis *et al.*, 2003). Cdc42 activation further stabilizes the AJs by linking VE-cadherin and α-ctn (Broman *et al.*, 2006). Given that VE-cadherin is linked to the actin cytoskeleton and that the Rho family GTPases regulate actin reorganization, VE-cadherin engagement might regulate the actin cytoskeleton. VE-cadherin inhibits cell proliferation by altering the actin cytoskeleton. This is achieved by altering, not only cell-cell contacts, but also cell-ECM contacts (Nelson and Chen, 2003).

Small GTPase Rap1-regulated VE-cadherin-dependent cell adhesion and VE-cadherin engagement-triggered Rap1 activation

In accordance with previous reports, we have reported that cAMP-Epac-Rap1 signal stabilizes adherens junction and thereby reduces cell permeability and decreases leukocyte migration (Wittchen *et al.*, 2005; Fukuhara *et al.*, 2005; Cullere *et al.*, 2005; Kooistra *et al.*, 2005). Rap1 is a small GTPase which belongs to the Ras family of proteins and is thought to antagonize Ras function by sharing Ras effector molecules such as c-Raf, RalGDS, and PI3-K. Recent data have revealed that Rap1 functions, not only as a Ras-competitor, but also as a cell adhesion regulator, particularly at the cell-ECM (Bos *et al.*, 2001; Bos *et al.*, 2003). Rap1 is activated by several guanine nucleotide exchange factors (GEF) which have regulatory motifs besides the catalytic domain.

Among GEFs for Rap1, we have focused on the effect of Epac, which is regulated by cAMP, on cell adhesion formation (Bos, 2003), because cAMP decreases cell permeability (Langeler and van Hinsbergh, 1991; Farmer *et al.*, 2001; Hippenstiel *et al.*, 2002). It has been reported that Rap1 activation is required for E-cadherin-based cell-cell contact formation (Hogan *et al.*, 2004; Price *et al.*, 2004). We and other groups have noticed that 007, a cAMP analogue (Cullere *et al.*, 2005) that directly activates Epac without activating protein kinase A, increases GTP-bound Rap1 and subsequently augments the endothelial cell barrier function. We reasoned that cAMP induces endothelial cortical actin rearrangement in a manner dependent on Rap1 activation. Although we have not identified the molecules that regulate actin cytoskeleton downstream of Rap1, increased bundling of cortical actin might support the VE-cadherin by linking VE-cadherin and actin via α- and β-ctn.

We explored the possibility that VE-cadherin engagement activates Rap1 (Sakurai *et al.*, 2006). As mentioned earlier, MAGI-1 is capable of binding to JAM. Moreover, MAGI-1 associates with β-ctn (Kotelevets *et al.*, 2005). MAGI-1 consists of 6 PSD95/ DiscLarge/ ZO-1 (PDZ) domains, a guanylate kinase domain and two WW domains flanked by the first and second PDZ domain (Dobrosotskaya *et al.*, 1997). Since PDZ domains are docking domains for PDZ-binding molecules, MAGI-1 associates with a variety molecules such as NMDA receptors, PTEN, BAI-1, mNET1, and PDZ-GEF1 (Mino *et al.*, 2000; Dobrosotskaya, 2001) (Kawajiri *et al.*, 2000) (Dobrosotskaya and James, 2000). PDZ-GEF1 is a GEF for Rap1. We hypothesized that MAGI-1-PDZ-GEF1 signal participates in the activation of Rap1 at the cell-cell contacts in vascular endothelial cells and that this signal is triggered upon cell-cell contact.

Rap1 is activated upon cell-cell contact in vascular endothelial cells as demonstrated by fluorescent resonance energy transfer (FRET)-based probe (Mochizuki *et al.*, 2001; Sakurai *et al.*, 2006). We therefore delineated the mechanism by which Rap1 is activated. VE-cadherin homophilic interaction induced Rap1 activation, because Ca^{2+}-chelating and restoring experiments showed Rap1 activation. Using FRET technique, we found that the dominant negative form of MAGI-1, which perturbs the localization of MAGI-1 to cell-cell contacts, inhibits Rap1 activation upon cell-cell contact. In addition, MAGI-1 depletion by knockdown using siRNA inhibited the Rap1 activation at the cell-cell contact. These results suggested that MAGI-1 is required for Rap1 activation.

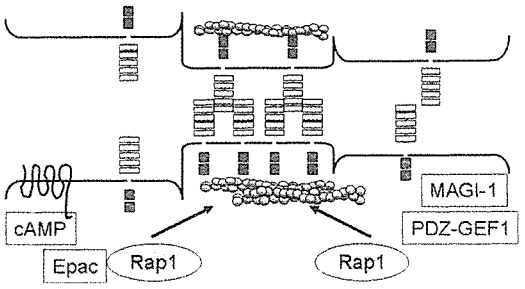

Fig. 2. Rap1 augments endothelial cell adhesion. Increase in cAMP upon G-protein-coupled receptor stimulation results in Epac-Rap1 activation, thereby inducing VE-cadherin-mediated cell adhesion. Homophilic VE-cadherin engagement also activates Rap1 via MAGI-1-PDZ-GEF1. Subsequently activated Rap1 results in rearranging actin cytoskeleton to support cell-cell adhesion.

We confirmed that MAGI-1 associates with β-ctn and PDZ-GEF1 in vascular endothelial cells.

Relocation of vinculin to cell-cell contacts from cell-ECM was hampered in MAGI-1-depleted cells, indicating that vinculin may function downstream of Rap1 for tightening cell-cell adhesion. Collectively, MAGI-1 linking β-ctn and PDZ-GEF1 is important for VE-cadherin-mediated Rap1 activation.

Rap1 activated by cAMP via Epac functions stabilizes VE-cadherin-dependent cell adhesion. Rap1 that is activated upon cell-cell contact via MAGI-1-PDZ-GEF1 also accelerates VE-cadherin-mediated cell adhesion. Thus, Rap1 regulates inside-out signal for VE-cadherin assembly. These data are summarized in Fig. 2.

Homophilic dimerization of nectin at the AJs triggers Rap1 activation via Src-Crk (Fukuyama *et al.*, 2005). Because both nectin and cadherin are present at the AJs, they coordinate AJ formation by activating Rap1. Afadin linking nectin to actin cytoskeleton appears to be a key effector molecule of activated Rap1. Although we have not yet found the direct effector of activated Rap1 upon VE-cadherin-mediated signal, both nectin- and VE-cadherin-triggered Rap1 activation results in the assembly of actin cytoskeleton. Conversely, both nectin and VE-cadherin might be supported by actin cytoskeleton.

VE-cadherin expression at the cell-cell adhesion controlled by trafficking and stabilization

VE-cadherin is not static at AJ and is endocytosed, degraded, and/or recycled by vesicular trafficking. VE-cadherin-mediated cell-cell adhesion is dynamically regulated by trafficking and stabilization at the cell-cell contacts. VE-cadherin appears to be processed by vesicular trafficking both from and to the plasma membrane, similar to E-cadherin (Bryant and Stow, 2004). However, the molecular mechanism of VE-cadherin endocytosis and exocytosis has not been completely elucidated.

Kowalczyk's group has recently reported that VE-cadherin is endocytosed in a manner dependent on clathrin (Xiao *et al.*, 2005). They reported that p120ctn inhibits VE-cadherin endocytosis. Previously, p120ctn has also been suggested to be involved in the exocytic pathway of cadherin-containing vesicles (Mary *et al.*, 2002; Peifer and Yap, 2003; Chen *et al.*, 2003). Given that the cytoplasmic domain of VE-cadherin is biochemically and structurally similar to E-cadherin, except for the absence of the di-Leu motif found in E-cadherin, VE-cadherin may enter the endocytosis pathway in a clathrin-independent manner (Akhtar and Hotchin, 2001; Paterson *et al.*, 2003).

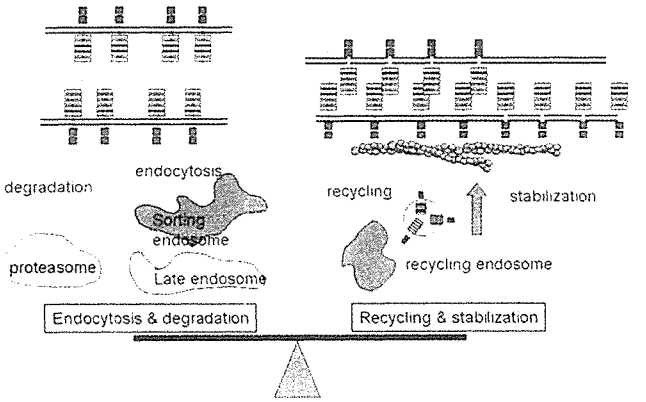

Fig. 3. VE-cadherin turnover and stabilization. Expression of VE-cadherin depends on the balance between VE-cadherin degradation/endocytosis and recycling/stabilization. Recent advance in cadherin biology has revealed the signaling cue for endocytosis and destabilization of VE-cadherin. Yet, we further need to clarify the cur for recycling and how VE-cadherin in endosomes is processed.

VE-cadherin biogenesis and turnover is not strictly analyzed yet, although half life of E-cadherin is suggested to be 2-5 hours (Gumbiner, 2000). Transcriptional regulation of VE-cadherin is not fully elucidated, although genomic organization of cadherin family genes are unraveled (Angst *et al.*, 2001). VE-cadherin is subjected to shedding by metalloproteinases (Herren *et al.*, 1998). The remaining molecules might be cleaved by γ-secretase as other classical cadherins are processed (Periz and Fortini, 2004).

Interestingly, nectin is one of the candidates as a substrate for γ-secretase (Kim *et al.*, 2002). An interesting paper demonstrated that a deficiency of Preselinin-1, a component of γ-secretase, results in abnormal vascular formation (Nakajima *et al.*, 2003). It will be interesting to study the function of the intracellular domain fragment cleaved by γ-secretase in the future. Although E-cadherin is processed by a ubiquitination pathway by Hakai (Pece and Gutkind, 2002), VE-cadherin lacks the ubiquitination site by Hakai. Thus, VE-cadherin may be degraded by alternative ubiquitination signaling.

As summarized in Fig. 3, the expression and function of VE-cadherin at the cell-cell contacts depends on the balance between internalization and stabilization. The internalized VE-cadherins are either degraded or recycled back to the membrane via trafficking and sorting signals.

Perspectives

Vascular endothelial cells have to assemble and disassemble during angiogenesis. In addition, cell adhesion is affected by the stretch induced by smooth muscle contraction and by the extravasation of blood cells. To understand how VE-cadherin-mediated cell adhesion is regulated in response to mechanical stress and biochemical signaling, we need to further study (1) what kind of stimuli controls VE-cadherin stabilization, (2) what kind of extracellular stimuli regulates the endocytosis and degradation of VE-cadherin, (3) which signals accelerate the recycling of VE-cadherin. The major unanswered question, however, relates to the cue for VE-cadherin trafficking to the plasma membrane. Recently p120ctn is involved in stabilizing VE-cadherin and trafficking of VE-cadherin (Vincent *et al.*, 2004) It will be interesting to investigate the signal that p120ctn responds in virtue of VE-cadherin regulation.

Acknowledgments We are grateful to Y. Matsuura for technical assistance, to D.O. Schwenke for critical reading of this review, and to Y.M. Kim for providing us with a chance to review VE-cadherin regulation. This work was supported by grants from the Ministry of Health, Labour, and Welfare Foundation of Japan, from the Program for Promotion of Fundamental Studies in Health Sciences of the National Institute of Biomedical Innovation, from the Ministry of Education, Science, Sports and Culture of Japan.

References

Adams, R. H. and Klein, R. (2000) Eph receptors and ephrin ligands. essential mediators of vascular development. *Trends Cardiovasc. Med.* **10**, 183-188.

Akhtar, N. and Hotchin, N. A. (2001) RAC1 regulates adherens junctions through endocytosis of E-cadherin. *Mol. Biol. Cell* **12**, 847-862.

Angst, B. D., Marcozzi, C. and Magee, A. I. (2001) The cadherin superfamily: diversity in form and function. *J. Cell Sci.* **114**, 629-641.

Bazzoni, G. (2003) The JAM family of junctional adhesion molecules. *Curr. Opin. Cell Biol.* **15**, 525-530.

Bos, J. L. (2003) Epac: a new cAMP target and new avenues in cAMP research. *Nat. Rev. Mol. Cell Biol.* **4**, 733-738.

Bos, J. L., de Bruyn, K., Enserink, J., Kuiperij, B., Rangarajan, S., Rehmann, H., Riedl, J., de Rooij, J., van Mansfeld, F. and Zwartkruis, F. (2003) The role of Rap1 in integrin-mediated cell adhesion. *Biochem. Soc. Trans.* **31**, 83-86.

Bos, J. L., de Rooij, J. and Reedquist, K. A. (2001) Rap1 signalling: adhering to new models. *Nat. Rev. Mol. Cell Biol.* **2**, 369-377.

Broman, M. T., Kouklis, P., Gao, X., Ramchandran, R., Neamu, R. F., Minshall, R. D. and Malik, A. B. (2006) Cdc42 regulates adherens junction stability and endothelial permeability by inducing alpha-catenin interaction with the vascular endothelial cadherin complex. *Circ. Res.* **98**, 73-80.

Bryant, D. M. and Stow, J. L. (2004) The ins and outs of E-cadherin trafficking. *Trends Cell Biol.* **14**, 427-434.

Carmeliet, P., Lampugnani, M. G., Moons, L., Breviario, F., Compernolle, V., Bono, F., Balconi, G., Spagnuolo, R., Oostuyse, B., Dewerchin, M., Zanetti, A., Angellilo, A., Mattot, V., Nuyens, D., Lutgens, E., Clotman, F., de Ruiter, M. C., Gittenberger-de Groot, A., Poelmann, R., Lupu, F., Herbert, J. M., Collen, D. and Dejana, E. (1999) Targeted deficiency or cytosolic truncation of the VE-cadherin gene in mice impairs VEGF-mediated endothelial survival and angiogenesis. *Cell* **98**, 147-157.

Caveda, L., Martin-Padura, I., Navarro, P., Breviario, F., Corada, M., Gulino, D., Lampugnani, M. G. and Dejana, E. (1996) Inhibition of cultured cell growth by vascular endothelial cadherin (cadherin-5/VE-cadherin). *J. Clin. Invest* **98**, 886-893.

Chappuis-Flament, S., Wong, E., Hicks, L. D., Kay, C. M. and Gumbiner, B. M. (2001) Multiple cadherin extracellular repeats mediate homophilic binding and adhesion. *J. Cell Biol.* **154**, 231-243.

Chen, X., Kojima, S., Borisy, G. G. and Green, K. J. (2003) p120 catenin associates with kinesin and facilitates the transport of cadherin-catenin complexes to intercellular junctions. *J. Cell Biol.* **163**, 547-557.

Cullere, X., Shaw, S. K., Andersson, L., Hirahashi, J., Luscinskas, F. W. and Mayadas, T. N. (2005) Regulation of vascular endothelial barrier function by Epac, a cAMP-activated exchange factor for Rap GTPase. *Blood* **105**, 1950-1955.

Davis, G. E. and Senger, D. R. (2005) Endothelial extracellular matrix: biosynthesis, remodeling, and functions during vascular morphogenesis and neovessel stabilization. *Circ. Res.* **97**, 1093-1107.

Dejana, E. (2004) Endothelial cell-cell junctions: happy together. *Nat. Rev. Mol. Cell Biol.* **5**, 261-270.

Dobrosotskaya, I., Guy, R. K. and James, G. L. (1997) MAGI-1, a membrane-associated guanylate kinase with a unique arrangement of protein-protein interaction domains. *J. Biol. Chem.* **272**, 31589-31597.

Dobrosotskaya, I. Y. (2001) Identification of mNET1 as a candidate ligand for the first PDZ domain of MAGI-1. *Biochem. Biophys. Res. Commun.* **283**, 969-975.

Dobrosotskaya, I. Y. and James, G. L. (2000) MAGI-1 interacts with beta-catenin and is associated with cell-cell adhesion structures. *Biochem. Biophys. Res. Commun.* **270**, 903-909.

Drees, F., Pokutta, S., Yamada, S., Nelson, W. J. and Weis, W. I. (2005) Alpha-catenin is a molecular switch that binds E-cadherin-beta-catenin and regulates actin-filament assembly. *Cell* **123**, 903-915.

Esser, S., Lampugnani, M. G., Corada, M., Dejana, E. and Risau, W. (1998) Vascular endothelial growth factor induces VE-cadherin tyrosine phosphorylation in endothelial cells. *J. Cell Sci.* **111**, 1853-1865.

Farmer, P. J., Bernier, S. G., Lepage, A., Guillemette, G., Regoli, D. and Sirois, P. (2001) Permeability of endothelial monolayers to albumin is increased by bradykinin and inhibited by prostaglandins. *Am. J. Physiol Lung Cell Mol. Physiol* **280**, 732-738.

Fong, G. H., Rossant, J., Gertsenstein, M. and Breitman, M. L. (1995) Role of the Flt-1 receptor tyrosine kinase in regulating the assembly of vascular endothelium. *Nature* **376**, 66-70.

Fukata, M. and Kaibuchi, K. (2001) Rho-family GTPases in cadherin-mediated cell-cell adhesion. *Nat. Rev. Mol. Cell Biol.*

2, 887-897.

Fukuhara, S., Sakurai, A., Sano, H., Yamagishi, A., Somekawa, S., Takakura, N., Saito, Y., Kangawa, K. and Mochizuki, N. (2005) Cyclic AMP potentiates vascular endothelial cadherin-mediated cell-cell contact to enhance endothelial barrier function through an Epac-Rap1 signaling pathway. *Mol. Cell Biol.* **25**, 136-146.

Fukuyama, T., Ogita, H., Kawakatsu, T., Fukuhara, T., Yamada, T., Sato, T., Shimizu, K., Nakamura, T., Matsuda, M. and Takai, Y. (2005) Involvement of the c-Src-Crk-C3G-Rap1 signaling in the nectin-induced activation of Cdc42 and formation of adherens junctions. *J. Biol. Chem.* **280**, 815-825.

Gale, N. W., Thurston, G., Hackett, S. F., Renard, R., Wang, Q., McClain, J., Martin, C., Witte, C., Witte, M. H., Jackson, D., Suri, C., Campochiaro, P. A., Wiegand, S. J. and Yancopoulos, G. D. (2002) Angiopoietin-2 is required for postnatal angiogenesis and lymphatic patterning, and only the latter role is rescued by Angiopoietin-1. *Dev. Cell* **3**, 411-423.

Gale, N. W. and Yancopoulos, G. D. (1999) Growth factors acting via endothelial cell-specific receptor tyrosine kinases: VEGFs, angiopoietins, and ephrins in vascular development. *Genes Dev.* **13**, 1055-1066.

Grazia, L. M., Zanetti, A., Corada, M., Takahashi, T., Balconi, G., Breviario, F., Orsenigo, F., Cattelino, A., Kemler, R., Daniel, T. O. and Dejana, E. (2003b) Contact inhibition of VEGF-induced proliferation requires vascular endothelial cadherin, beta-catenin, and the phosphatase DEP-1/CD148. *J. Cell Biol.* **161**, 793-804.

Grazia, L. M., Zanetti, A., Corada, M., Takahashi, T., Balconi, G., Breviario, F., Orsenigo, F., Cattelino, A., Kemler, R., Daniel, T. O. and Dejana, E. (2003a) Contact inhibition of VEGF-induced proliferation requires vascular endothelial cadherin, beta-catenin, and the phosphatase DEP-1/CD148. *J. Cell Biol.* **161**, 793-804.

Gumbiner, B., Lowenkopf, T. and Apatira, D. (1991) Identification of a 160-kDa polypeptide that binds to the tight junction protein ZO-1. *Proc. Natl. Acad. Sci. USA* **88**, 3460-3464.

Gumbiner, B. M. (2000) Regulation of cadherin adhesive activity. *J. Cell Biol.* **148**, 399-404.

Herren, B., Levkau, B., Raines, E. W. and Ross, R. (1998) Cleavage of beta-catenin and plakoglobin and shedding of VE-cadherin during endothelial apoptosis: evidence for a role for caspases and metalloproteinases. *Mol. Biol. Cell* **9**, 1589-1601.

Hippenstiel, S., Witzenrath, M., Schmeck, B., Hocke, A., Krisp, M., Krull, M., Seybold, J., Seeger, W., Rascher, W., Schutte, H. and Suttorp, N. (2002) Adrenomedullin reduces endothelial hyperpermeability. *Circ. Res.* **91**, 618-625.

Hogan, C., Serpente, N., Cogram, P., Hosking, C. R., Bialucha, C. U., Feller, S. M., Braga, V. M., Birchmeier, W. and Fujita, Y. (2004) Rap1 regulates the formation of E-cadherin-based cell-cell contacts. *Mol. Cell Biol.* **24**, 6690-6700.

Hudry-Clergeon, H., Stengel, D., Ninio, E. and Vilgrain, I. (2005) Platelet-activating factor increases VE-cadherin tyrosine phosphorylation in mouse endothelial cells and its association with the PtdIns3'-kinase. *FASEB J.* **19**, 512-520.

Jackson, D. E., Ward, C. M., Wang, R. and Newman, P. J. (1997) The protein-tyrosine phosphatase SHP-2 binds platelet/endothelial cell adhesion molecule-1 (PECAM-1) and forms a distinct signaling complex during platelet aggregation. Evidence for a mechanistic link between PECAM-1- and integrin-mediated cellular signaling. *J. Biol. Chem.* **272**, 6986-6993.

Kawajiri, A., Itoh, N., Fukata, M., Nakagawa, M., Yamaga, M., Iwamatsu, A. and Kaibuchi, K. (2000) Identification of a novel beta-catenin-interacting protein. *Biochem. Biophys. Res. Commun.* **273**, 712-717.

Keck, P. J., Hauser, S. D., Krivi, G., Sanzo, K., Warren, T., Feder, J. and Connolly, D. T. (1989) Vascular permeability factor, an endothelial cell mitogen related to PDGF. *Science* **246**, 1309-1312.

Kim, D. Y., Ingano, L. A. and Kovacs, D. M. (2002) Nectin-1alpha, an immunoglobulin-like receptor involved in the formation of synapses, is a substrate for presenilin/gamma-secretase-like cleavage. *J. Biol. Chem.* **277**, 49976-49981.

Kooistra, M. R., Corada, M., Dejana, E. and Bos, J. L. (2005) Epac1 regulates integrity of endothelial cell junctions through VE-cadherin. *FEBS Lett.* **579**, 4966-4972.

Kotelevets, L., van Hengel, J., Bruyneel, E., Mareel, M., van Roy, F. and Chastre, E. (2005) Implication of the MAGI-1b/PTEN signalosome in stabilization of adherens junctions and suppression of invasiveness. *FASEB J.* **19**, 115-117.

Kouklis, P., Konstantoulaki, M. and Malik, A. B. (2003) VE-cadherin-induced Cdc42 signaling regulates formation of membrane protrusions in endothelial cells. *J. Biol. Chem.* **278**, 16230-16236.

Kovacs, E. M., Ali, R. G., McCormack, A. J. and Yap, A. S. (2002) E-cadherin homophilic ligation directly signals through Rac and phosphatidylinositol 3-kinase to regulate adhesive contacts. *J. Biol. Chem.* **277**, 6708-6718.

Lambeng, N., Wallez, Y., Rampon, C., Cand, F., Christe, G., Gulino-Debrac, D., Vilgrain, I. and Huber, P. (2005) Vascular endothelial-cadherin tyrosine phosphorylation in angiogenic and quiescent adult tissues. *Circ. Res.* **96**, 384-391.

Lampugnani, M. G., Corada, M., Caveda, L., Breviario, F., Ayalon, O., Geiger, B. and Dejana, E. (1995) The molecular organization of endothelial cell to cell junctions: differential association of plakoglobin, beta-catenin, and alpha-catenin with vascular endothelial cadherin (VE-cadherin). *J. Cell Biol.* **129**, 203-217.

Langeler, E. G. and van Hinsbergh, V. W. (1991) Norepinephrine and iloprost improve barrier function of human endothelial cell monolayers: role of cAMP. *Am. J. Physiol.* **260**, 1052-1059.

Laura, R. P., Ross, S., Koeppen, H. and Lasky, L. A. (2002) MAGI-1: a widely expressed, alternatively spliced tight junction protein. *Exp. Cell Res.* **275**, 155-170.

Luo, Y. and Radice, G. L. (2005) N-cadherin acts upstream of VE-cadherin in controlling vascular morphogenesis. *J. Cell Biol.* **169**, 29-34.

Mary, S., Charrasse, S., Meriane, M., Comunale, F., Travo, P., Blangy, A. and Gauthier-Rouviere, C. (2002) Biogenesis of N-cadherin-dependent cell-cell contacts in living fibroblasts is a microtubule-dependent kinesin-driven mechanism. *Mol. Biol. Cell* **13**, 285-301.

Masuda, M., Osawa, M., Shigematsu, H., Harada, N. and Fujiwara, K. (1997) Platelet endothelial cell adhesion molecule-1 is a major SH-PTP2 binding protein in vascular endothelial cells. *FEBS Lett.* **408**, 331-336.

Mino, A., Ohtsuka, T., Inoue, E. and Takai, Y. (2000) Membrane-associated guanylate kinase with inverted orientation (MAGI)-1/brain angiogenesis inhibitor 1-associated protein (BAP1) as a scaffolding molecule for Rap small G protein GDP/GTP

exchange protein at tight junctions. *Genes Cells* **5**, 1009-1016.

Mochizuki, N., Yamashita, S., Kurokawa, K., Ohba, Y., Nagai, T., Miyawaki, A. and Matsuda, M. (2001) Spatio-temporal images of growth-factor-induced activation of Ras and Rap1. *Nature* **411**, 1065-1068.

Nagashima, K., Endo, A., Ogita, H., Kawana, A., Yamagishi, A., Kitabatake, A., Matsuda, M. and Mochizuki, N. (2002) Adaptor protein Crk is required for Ephrin-B1-induced membrane ruffling and focal complex assembly of human aortic endothelial cells. *Mol. Biol. Cell* **13**, 4231-4242.

Nakajima, M., Yuasa, S., Ueno, M., Takakura, N., Koseki, H. and Shirasawa, T. (2003) Abnormal blood vessel development in mice lacking presenilin-1. *Mech. Dev.* **120**, 657-667.

Navarro, P., Ruco, L. and Dejana, E. (1998) Differential localization of VE- and N-cadherins in human endothelial cells: VE-cadherin competes with N-cadherin for junctional localization. *J. Cell Biol.* **140**, 1475-1484.

Nelson, C. M. and Chen, C. S. (2003) VE-cadherin simultaneously stimulates and inhibits cell proliferation by altering cytoskeletal structure and tension. *J. Cell Sci.* **116**, 3571-3581.

Newman, P. J. and Newman, D. K. (2003) Signal transduction pathways mediated by PECAM-1: new roles for an old molecule in platelet and vascular cell biology. *Arterioscler. Thromb. Vasc. Biol.* **23**, 953-964.

Nwariaku, F. E., Liu, Z., Zhu, X., Nahari, D., Ingle, C., Wu, R. F., Gu, Y., Sarosi, G. and Terada, L. S. (2004) NADPH oxidase mediates vascular endothelial cadherin phosphorylation and endothelial dysfunction. *Blood* **104**, 3214-3220.

Osawa, M., Masuda, M., Kusano, K. and Fujiwara, K. (2002) Evidence for a role of platelet endothelial cell adhesion molecule-1 in endothelial cell mechanosignal transduction: is it a mechanoresponsive molecule? *J. Cell Biol.* **158**, 773-785.

Paterson, A. D., Parton, R. G., Ferguson, C., Stow, J. L. and Yap, A. S. (2003) Characterization of E-cadherin endocytosis in isolated MCF-7 and chinese hamster ovary cells: the initial fate of unbound E-cadherin. *J. Biol. Chem.* **278**, 21050-21057.

Pece, S. and Gutkind, J. S. (2002) E-cadherin and Hakai: signalling, remodeling or destruction? *Nat. Cell Biol.* **4**, 72-74.

Peifer, M. and Yap, A. S. (2003) Traffic control: p120-catenin acts as a gatekeeper to control the fate of classical cadherins in mammalian cells. *J. Cell Biol.* **163**, 437-440.

Periz, G. and Fortini, M. E. (2004) Functional reconstitution of gamma-secretase through coordinated expression of presenilin, nicastrin, Aph-1, and Pen-2. *J. Neurosci. Res.* **77**, 309-322.

Potter, M. D., Barbero, S. and Cheresh, D. A. (2005) Tyrosine phosphorylation of VE-cadherin prevents binding of p120- and beta-catenin and maintains the cellular mesenchymal state. *J. Biol. Chem.* **280**, 31906-31912.

Price, L. S., Hajdo-Milasinovic, A., Zhao, J., Zwartkruis, F. J., Collard, J. G. and Bos, J. L. (2004) Rap1 regulates E-cadherin-mediated cell-cell adhesion. *J. Biol. Chem.* **279**, 35127-35132.

Rahimi, N. and Kazlauskas, A. (1999) A role for cadherin-5 in regulation of vascular endothelial growth factor receptor 2 activity in endothelial cells. *Mol. Biol. Cell* **10**, 3401-3407.

Reymond, N., Imbert, A. M., Devilard, E., Fabre, S., Chabannon, C., Xerri, L., Farnarier, C., Cantoni, C., Bottino, C., Moretta, A., Dubreuil, P. and Lopez, M. (2004) DNAM-1 and PVR regulate monocyte migration through endothelial junctions. *J. Exp. Med.* **199**, 1331-1341.

Sakisaka, T. and Takai, Y. (2004) Biology and pathology of nectins and nectin-like molecules. *Curr. Opin. Cell Biol.* **16**, 513-521.

Sakurai, A., Fukuhara, S., Yamagishi, A., Sako, K., Kamioka, Y., Masuda, M., Nakaoka, Y. and Mochizuki, N. (2006) MAGI-1 is required for Rap1 activation upon cell-cell contact and for enhancement of vascular endothelial cadherin-mediated cell adhesion. *Mol. Biol. Cell* **17**, 966-976.

Salomon, D., Ayalon, O., Patel-King, R., Hynes, R. O. and Geiger, B. (1992) Extrajunctional distribution of N-cadherin in cultured human endothelial cells. *J. Cell Sci.* **102**, 7-17.

Shalaby, F., Rossant, J., Yamaguchi, T. P., Gertsenstein, M., Wu, X. F., Breitman, M. L., and Schuh, A. C. (1995) Failure of blood-island formation and vasculogenesis in Flk-1-deficient mice. *Nature* **376**, 62-66.

Shay-Salit, A., Shushy, M., Wolfovitz, E., Yahav, H., Breviario, F., Dejana, E. and Resnick, N. (2002) VEGF receptor 2 and the adherens junction as a mechanical transducer in vascular endothelial cells. *Proc. Natl. Acad. Sci. USA* **99**, 9462-9467.

Shoji, H., Tsuchida, K., Kishi, H., Yamakawa, N., Matsuzaki, T., Liu, Z., Nakamura, T. and Sugino, H. (2000) Identification and characterization of a PDZ protein that interacts with activin type II receptors. *J. Biol. Chem.* **275**, 5485-5492.

Suri, C., Jones, P. F., Patan, S., Bartunkova, S., Maisonpierre, P. C., Davis, S., Sato, T. N. and Yancopoulos, G. D. (1996) Requisite role of angiopoietin-1, a ligand for the TIE2 receptor, during embryonic angiogenesis. *Cell* **87**, 1171-1180.

Takai, Y. and Nakanishi, H. (2003) Nectin and afadin: novel organizers of intercellular junctions. *J. Cell Sci.* **116**, 17-27.

Telo', P., Breviario, F., Huber, P., Panzeri, C. and Dejana, E. (1998) Identification of a novel cadherin (vascular endothelial cadherin-2) located at intercellular junctions in endothelial cells. *J. Biol. Chem.* **273**, 17565-17572.

Tsukita, S., Furuse, M. and Itoh, M. (2001) Multifunctional strands in tight junctions. *Nat. Rev. Mol. Cell Biol.* **2**, 285-293.

Ukropec, J. A., Hollinger, M. K., Salva, S. M. and Woolkalis, M. J. (2000) SHP2 association with VE-cadherin complexes in human endothelial cells is regulated by thrombin. *J. Biol. Chem.* **275**, 5983-5986.

Vincent, P. A., Xiao, K., Buckley, K. M. and Kowalczyk, A. P. (2004) VE-cadherin: adhesion at arm's length. *Am. J. Physiol Cell Physiol* **286**, 987-997.

Wegmann, F., Ebnet, K., Du, P. L., Vestweber, D. and Butz, S. (2004) Endothelial adhesion molecule ESAM binds directly to the multidomain adaptor MAGI-1 and recruits it to cell contacts. *Exp. Cell Res.* **300**, 121-133.

Weis, S., Shintani, S., Weber, A., Kirchmair, R., Wood, M., Cravens, A., McSharry, H., Iwakura, A., Yoon, Y. S., Himes, N., Burstein, D., Doukas, J., Soll, R., Losordo, D. and Cheresh, D. (2004) Src blockade stabilizes a Flk/cadherin complex, reducing edema and tissue injury following myocardial infarction. *J. Clin. Invest* **113**, 885-894.

Wheelock, M. J. and Johnson, K. R. (2003) Cadherin-mediated cellular signaling. *Curr. Opin. Cell Biol.* **15**, 509-514.

Wittchen, E. S., Worthylake, R. A., Kelly, P., Casey, P. J., Quilliam, L. A. and Burridge, K. (2005) Rap1 GTPase inhibits leukocyte transmigration by promoting endothelial barrier function. *J. Biol. Chem.* **280**, 11675-11682.

Wong, V. and Gumbiner, B. M. (1997) A synthetic peptide corresponding to the extracellular domain of occludin perturbs

the tight junction permeability barrier. *J. Cell Biol.* **136**, 399-409.

Xiao, K., Garner, J., Buckley, K. M., Vincent, P. A., Chiasson, C. M., Dejana, E., Faundez, V. and Kowalczyk, A. P. (2005) p120-Catenin regulates clathrin-dependent endocytosis of VE-cadherin. *Mol. Biol. Cell* **16**, 5141-5151.

Yamada, S., Pokutta, S., Drees, F., Weis, W. I. and Nelson, W. J. (2005) Deconstructing the cadherin-catenin-actin complex. *Cell* **123**, 889-901.

Yancopoulos, G. D., Davis, S., Gale, N. W., Rudge, J. S., Wiegand, S. J. and Holash, J. (2000) Vascular-specific growth factors and blood vessel formation. *Nature* **407**, 242-248.

Zanetti, A., Lampugnani, M. G., Balconi, G., Breviario, F., Corada, M., Lanfrancone, L. and Dejana, E. (2002) Vascular endothelial growth factor induces SHC association with vascular endothelial cadherin: a potential feedback mechanism to control vascular endothelial growth factor receptor-2 signaling. *Arterioscler. Thromb. Vasc. Biol.* **22**, 617-622.

The EMBO Journal (2006) 25, 2889–2897 | © 2006 European Molecular Biology Organization | All Rights Reserved 0261-4189/06
www.embojournal.org

THE EMBO JOURNAL

Endophilin BAR domain drives membrane curvature by two newly identified structure-based mechanisms

Michitaka Masuda[1,4], Soichi Takeda[2,3,4], Manami Sone[1], Takashi Ohki[1], Hidezo Mori[2], Yuji Kamioka[1] and Naoki Mochizuki[1,*]

[1]Department of Structural Analysis, National Cardiovascular Center Research Institute, Suita, Osaka, Japan, [2]Department of Cardiac Physiology, National Cardiovascular Center Research Institute, Suita, Osaka, Japan and [3]Laboratory of structural biochemistry, RIKEN Harima Institute at SPring-8, Mikazuki-cho, Sayo, Hyogo, Japan

The crescent-shaped BAR (Bin/Amphiphysin/Rvs-homology) domain dimer is a versatile protein module that senses and generates positive membrane curvature. The BAR domain dimer of human endophilin-A1, solved at 3.1 Å, has a unique structure consisting of a pair of helix–loop appendages sprouting out from the crescent. The appendage's short helices form a hydrophobic ridge, which runs across the concave surface at its center. Examining liposome binding and tubulation *in vitro* using purified BAR domain and its mutants indicated that the ridge penetrates into the membrane bilayer and enhances liposome tubulation. BAR domain-expressing cells exhibited marked plasma membrane tubulation *in vivo*. Furthermore, a swinging-arm mutant lost liposome tubulation activity yet retaining liposome binding. These data suggested that the rigid crescent dimer shape is crucial for the tubulation. We here propose that the BAR domain drives membrane curvature by coordinate action of the crescent's scaffold mechanism and the ridge's membrane insertion in addition to membrane binding via amino-terminal amphipathic helix.

The EMBO Journal (2006) **25**, 2889–2897. doi:10.1038/sj.emboj.7601176; Published online 8 June 2006
Subject Categories: membranes & transport; structural biology
Keywords: BAR domain; endophilin; liposome; membrane curvature; membrane insertion

Introduction

Membrane dynamics in a cell, such as membrane budding, tubulation, fission and fusion, is associated with changes in membrane curvature. The crystal structure of amphiphysin BAR (Bin/Amphiphysin/Rvs-homology) domain revealed an unexpected structural identity with arfaptin2, a binding protein to Arf and Rac small GTPases (Tarricone *et al*, 2001), and provided a common structural base for the sensing and the formation of positive curvature membrane by BAR-family proteins (Peter *et al*, 2004).

Endophilins are cytoplasmic proteins containing an N-terminal BAR domain and a C-terminal SH3 domain, and are involved in membrane dynamics (Schuske *et al*, 2003; Galli and Haucke, 2004; Wenk and De Camilli, 2004). There are five endophilin genes in the mammalian genomes, endophilin A1–3 and B1–2. Both A and B types are highly conserved from nematode to human. The most extensively studied one is endophilin-A1, a brain specific protein involved in clathrin-mediated synaptic vesicle endocytosis (Ringstad *et al*, 1997, 2001). Via SH3 domain, endophilins bind to the GTPase dynamin, a membrane scissor, and the polyphosphoinositide phosphatase synaptojanin, a clathrin-uncoater (Ringstad *et al*, 1997; de Heuvel *et al*, 1997; Verstreken *et al*, 2003). The BAR domain of endophilins is classified into the N-BAR subgroup characterized by a short amphipathic helical sequence preceding the consensus BAR-domain sequence (Peter *et al*, 2004). The N-BAR domain of endophilin-A1 binds to liposomes and induces the tubulation *in vitro*, requiring the short amphipathic helical sequence (Farsad *et al*, 2001).

The crescent-shaped BAR dimer structure implies a simple model to drive membrane curvature: the dimer may impress its positively charged concave surface on the negatively charged membrane to form a high-curvature membrane domain (Gallop and McMahon, 2005; McMahon and Gallop, 2005). This curvature-impressing or scaffold mechanism for membrane deformation is based on an assumption that the dimer behaves as a rigid body on the membrane (Zimmerberg and Kozlov, 2006). Although the essential requirement of positively charged residues on the concave surface has been suggested (McMahon and Mills, 2004; Peter *et al*, 2004), there have been no experimental supports for the scaffold mechanism. Here, we show the requirement of the molecular rigidity of the BAR dimer for membrane curvature on the basis of structure-oriented mutational analysis.

By determining the structure of endophilin-A1 BAR domain, we found a distinction from those of the known BAR domains: a helix–loop appendage of 30 amino acids stretch is inserted into the helix I of the canonical BAR domain. A pair of the helices of the appendages forms a hydrophobic ridge, which runs across the center of the concave surface of the dimer. We analyzed the function of this ridge as well as the previously proposed structure, the N-terminal amphipathic helix and the crescent main body, for membrane deformation (Peter *et al*, 2004). N-terminal amphipathic helix is essential for membrane binding. The crescent main body of the BAR dimer is required for impressing its intrinsic curvature to the membrane. The ridge contributes to deform the membrane

*Corresponding author. Department of Structural Analysis, National Cardiovascular Center Research Institute, 5-7-1 Fujishiro-dai, Suita, Osaka 565-8565, Japan. Tel.: +81 6 6833 5012; Fax: +81 6 6835 5461; E-mail: nmochizu@ri.ncvc.go.jp
[4]These authors contributed equally to this work

Received: 15 November 2005; accepted: 8 May 2006; published online: 8 June 2006

©2006 European Molecular Biology Organization

presumably by penetrating into the membrane. Our results illustrate how these three components coordinate to induce membrane deformation.

Results

Endophilin-A1 BAR domain has a unique appendage

The structure of the BAR domain of human endophilin-A1 (amino acid 1–247, hereafter EndA1-BAR) was solved at 3.1 Å resolution by a multi-wavelength anomalous dispersion method. The structure of EndA1-BAR dimer is similar to that of amphiphysin (Peter *et al*, 2004) and arfaptin2 (Tarricone *et al*, 2001): a crescent-shaped dimer composed of a 6-helix bundle core and two 3-helix bundle arms extended from the core (Figure 1A). The whole structure of EndA1-BAR dimer can be precisely superimposed on that of amphiphysin and arfaptin (Figure 1B). All three structures show nearly identical dimer shapes. Notably, the present EndA1-BAR structure from a tetragonal crystal packing is almost completely the same as an independent crystal structure from an orthogonal crystal packing (Supplementary Figure 1; and Weissenhorn, 2005). The RMS deviations are 0.63, 0.86 and 0.80 Å for Cα atoms in monomers A, B and dimer, respectively. The structural identity indicates that the crescent shape is stably present in solution. Consistent with previous results (Habermann, 2004; Peter *et al*, 2004), structure-based sequence alignment reveals that these three proteins are poorly conserved in amino-acid sequence including the residues possibly important for the crescent-shape formation (Supplementary Figure 2).

We find a unique structure of the EndA1-BAR, an appendage-like structure protruded from the center of the dimer (Figure 1A). The sequence alignments of the BAR-family proteins indicated that this appendage appears unique to the endophilin-family proteins including nadrin (Habermann, 2004; Peter *et al*, 2004) and the candidates from yeasts (Supplementary Figure 2). The appendage (Q59–Q88) has an N-terminal short helix and a loop of which electron density is mostly missing (N72–G85). The pair of helices appears to stay on the main body and forms a ridge across the center of the concave dimer surface. The helix displays, on its top surface, a series of hydrophobic residues (P62, A63, A66 and M70) aligned 60° against the longitudinal axis of the dimer (Figure 1C). Other than the conserved hydrophobic amino acids of the ridge, the appendage sequences show clear distinction between endophilin-A and endophilin-B (Supplementary Figure 2). The B type endophilins show cytoplasmic localization, presumably being involved in intracellular membrane dynamics (Farsad *et al*, 2001; Modregger *et al*, 2003; Karbowski *et al*, 2004). Analyses of chimeric mutations in the appendage between EndA1-BAR and EndB1-BAR suggest that BAR domain may contribute to defining where to target, plasma membrane or intracellular organ membrane (Supplementary Figure 3).

The appendage's penetration enhances liposome tubulation

To investigate the functional significance of the hydrophobic ridge of the endophilin-specific appendage, we first examined the effects of point mutations in this region (red residues in Figure 1C) on the liposome binding and tubulation activities *in vitro* (Figures 2A and 3). Introduction of membrane-repulsive negative charge (A66D) lost the ability to form tubes from liposomes. Hydrophilic mutations (A63S/A66S (SS) and A63S/A66S/M70Q (SSQ)) reduced the number of tubes (<1/100) and induced three-time enlargement of the tube diameter. In contrast, a bulky hydrophobic residue

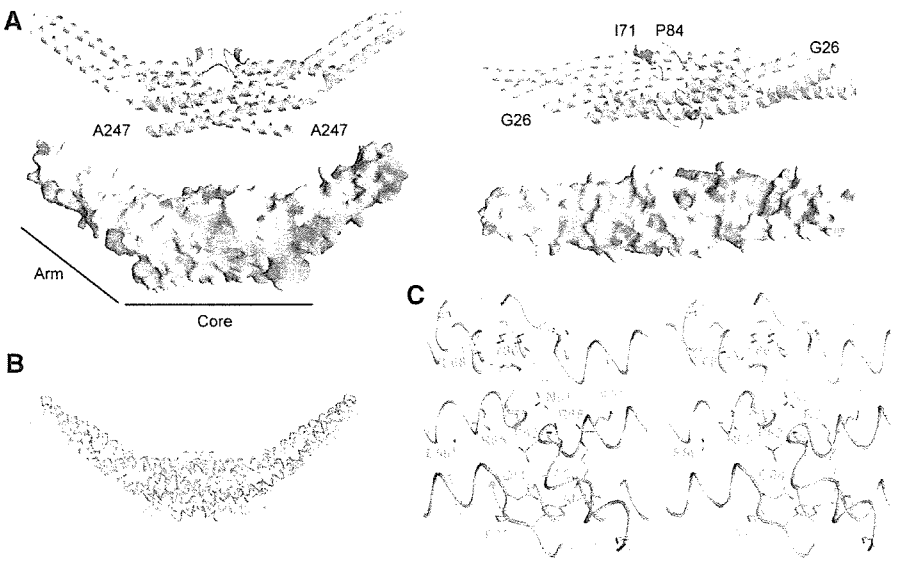

Figure 1 Structure of human endophilin-A1 BAR domain dimer. (**A**) Ribbon representation (a green monomer with a red appendage and a pale-blue monomer with a blue appendage) and surface electrostatic potential (red, $-15\,kTe^{-1}$; blue, $15\,kTe^{-1}$) of the dimer viewed from the side (left) and from the top (right). The numbered amino-acid residues are the first and the last ones in consecutive polypeptide segments determined in this model. (**B**) Comparison of three BAR domain structures in trace representation. Red, endophilin-A1 (PDB ID: 1X03); green, amphiphysin (1URU); blue, arfaptin2 (1I4D). The red and green arcs with indicated diameters represent curved membranes fit the concave surface of endophilin-A1 and amphiphysin, respectively. (**C**) Stereo view of the appendages. Side-chains of the residues forming the hydrophobic ridge and those of interacting with residues of the main body are shown.

 ©2006 European Molecular Biology Organization

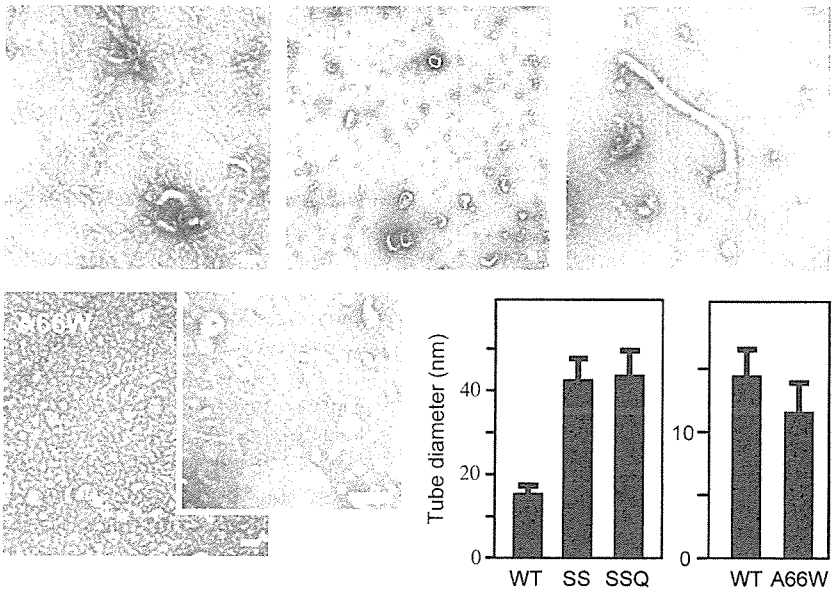

Figure 2 Liposome tubulation by endophilin-A1 BAR domains with mutations in the hydrophobic ridge. WT, 7 μM wild-type BAR domain incubated for 10 min; A66D, 28 μM, 10 min; SSQ, A63S/A66S/M70Q triple mutant, 28 μM, 10 min; A66W, 1.4 μM, 10 min (vesiculated, left panel) and 10 s (tubulated, right panel). Tubulation was not observed when incubated for longer than 1 min. Scale, 100 nm. The bar graphs show tubule diameter (mean and s.d.). SS, A63S/A66S double mutant, 28 μM, 10 min.

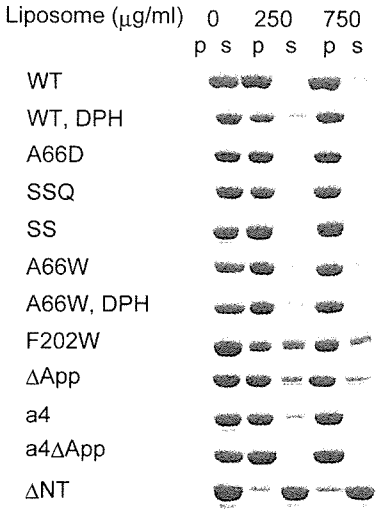

Figure 3 Liposome binding assays of endophilin-A1 BAR domain and its mutants. Protein (200 μg/ml) was co-sedimented with liposomes (0, 250 and 750 μg/ml). Proteins recovered from the pellet (p) and the supernatant (s) were analyzed by SDS–PAGE. The DPH-liposomes show similar binding capacity for the wild type (WT) and the A66W mutants. The liposome binding activity is slightly reduced in the F202W and the appendage-less mutants (ΔApp) and is almost lost in the helix 0 truncated mutant (ΔNT).

(A66W) led to extensive vesiculation and less tubulation. All these mutations did not affect the liposome binding. These results suggest an important role for the hydrophobic ridge in the membrane curvature formation but not in the membrane binding.

Although the ridge reduces the intrinsic curvature of the concave surface (red line in Figure 1B), it appears to promote the membrane curvature formation with conserved hydrophobicity. This raises the possibility that the ridge penetrates into the membrane when the concave surface makes tight contact with the membrane. This possibility was investigated using tryptophan fluorescence, which is sensitive to hydrophobicity of the microenvironment around the indole moiety. The A66W mutant showed 10-nm blueshift of the fluorescence peak in a liposome-dose-dependent and saturable manner, while F202W, a control mutant in which Phe202 on the convex surface was mutated to Trp, did not show any shift (Figure 4A and Supplementary Figure 5). The amount of the blueshift was greater than that observed in 50% DMSO or 50% methanol, indicating that the indol moiety was in a highly hydrophobic environment.

To determine whether this blueshift was caused by the insertion of the indol moiety into the hydrophobic core of the lipid bilayer, we made fluorescence resonance energy transfer (FRET) assays using diphenyl-hexatriene (DPH) as the acceptor probe. DPH has been shown to insert specifically in the nonpolar interior of the membrane and not to alter the membrane structure and dynamics (Repáková *et al*, 2005). DPH liposomes did not affect liposome binding and tubulation (Figure 3 and Supplementary Figure 4). A66W but not F202W showed effective FRET from the 340-nm tryptophan fluorescence (donar) to the DPH fluorescence (acceptor) peaked at 430 nm (Figure 4B and C). It was not caused by changes in the fluorescence property of DPH itself possibly accompanied by tubulation/vesiculation of liposomes (Figure 4D and Supplementary Figure 6). These data suggest that the indol ring of 66W penetrates into the hydrophobic core of the membrane and that the remaining residues of the ridge, about 8 Å in height, appear to be embedded in the layer of lipid head-groups of the contacting membrane leaflet. These results confirmed that the ridge is contacting membrane and that the convex is not contacting membrane surface.

To provide further support for the membrane insertion of the ridge in the wild-type EndA1-BAR, we made a mutant

©2006 European Molecular Biology Organization

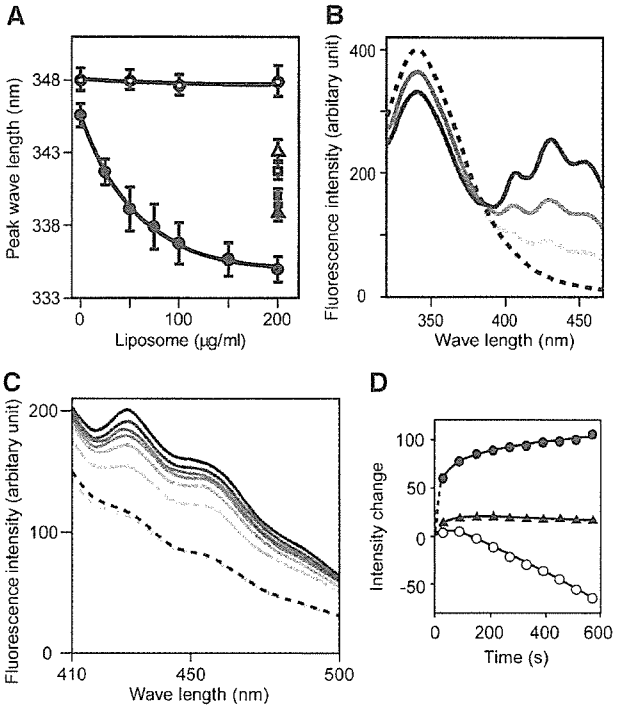

Figure 4 Tryptophan fluorescence blueshift and FRET assays. (**A**) Tryptophan fluorescence emission peak when excited at 280 nm was observed in different concentration of liposome. A66W (●), F202W control mutant (○), A66W alone in 50% DMSO (▲), in 50% MeOH (■), F202W alone in 50% DMSO (△), in 50% MeOH (□), 140 μg/ml protein for all measurements. Mean and s.d. ($N=4$–11). The dose dependency is significant ($P \ll 0.001$) for the A66W mutant but insignificant ($P > 0.8$) for the F202W mutant (one-way ANOVA). DMSO and MeOH were used as blueshift inducer for tryptophan. (**B**) Dose-dependent FRET efficiency from the A66W tryptophan to DPH incorporated in liposomes was examined by the changes of fluorescence. Fluorescence spectrum of A66W (100 μg/ml) with the control liposome (200 μg/ml) excited at 280 nm (hatched). Pale to dark solid curves represent DPH:lipid weight ratios of 1:2000, 1:1000 and 1:500 in the same condition. (**C**) Time-dependent increase in the FRET efficiency from either A66W (pale to dark solid lines, from 30 to 570 s) or F202W tryptophan (pale and dark hatched lines, at 30 and 570 s) to DPH incorporated in liposomes. DPH:lipid weight ratio is 1:500. (**D**) The intensity changes at the 430-nm peak are plotted against time. A66W (●), F202W (▲) excited at 280 nm and A66W (○) excited at 360 nm.

with amphiphysin/arfaptin shape and examined its tubulation activity. The mutant (ΔApp), in which the entire appendage (Q59–Q88) was replaced with a helical stretch (AHLSSLLQ) derived from arfaptin2 sequence (A152–Q159, Y155S), show the crystal structure of a canonical BAR-domain dimer as designed (Figure 5A and Supplementary Figure 7). The ΔApp could bind to liposomes (Figure 3) and cause tubulation to a lesser extent than the wild type and amphiphysin-BAR (Figure 5D and Supplementary Figure 4). As the diameter of the tubules reflects the membrane curvature if the section of the tube is circle, we measured the diameter of the tube to compare the curvature of the EndA1-BAR and its mutant-induced tubes. Despite the higher curvature of the concave surface, the ΔApp dimer induced larger diameter tubules than the wild type did, indicating a positive contribution of the wild-type hydrophobic ridge to drive membrane curvature. Taken all together, the hydrophobic ridge penetrates into the interfacial leaflet of the lipid bilayer when the concave surface is in contact with the membrane and promotes membrane curvature formation.

The BAR domain is rigid enough to impose its intrinsic curvature on membrane

A simple model for the concave surface-driven mechanism is that each BAR domain dimer acts as a molecular mold that impresses its curved surface on the membrane. This model suggests that the membrane curvature approximately mirrors the curvature of the concave surface. Indeed, the diameters of tubules induced by amphiphysin, ΔApp (Figure 5D), SS and SSQ mutants (Figure 2) are compatible with the model-based prediction (see Supplementary Table II for statistical analysis). However, this model has an assumption that the dimer should be rigid enough to overcome the bending resistance of the membrane (Nossal and Zimmerberg, 2002; Farsad and De Camilli, 2003). To examine whether the molecular mold mechanism is feasible, we developed a straight BAR domain by inserting one helical pitch into the helix II in the proximal portion of the extending arm (QSAL is inserted between I154 and Q155). This mutation (a4) would compensate the unequal lengths between helix II and III in the arm, a common feature of the known BAR domain structures, and let the curved arm into a straight one. Although the a4 mutant was designed simply to straighten the curvature of the domain, the structure solved at 2.4 Å resolution shows that it actually has the very interesting property of a flexible arm rather than a rigid one (Figure 5B). Four monomers in the asymmetrical unit show deviation in the bending angles of arms. The blue and the green monomers have straight arms while the orange monomer shows a bending pattern similar to the wild type and the yellow monomer is an intermediate. The structural deviation almost exclusively occurs in the helix kink regions (Supplementary Figure 8), indicating that the arm can swing at least from the bend-free straight position to nearly the wild-type position.

The a4 mutant allowed us to examine how flexibility of the crescent-shaped main body of the BAR dimer affects the membrane curvature formation. The insertion of one helical pitch slightly distorts relative position of the helix II and III (Figure 5C), but does not largely rearrange the spatial positions of the residues on the concave surface of the arm (Supplementary Figure 8). Indeed, the a4 mutant and its appendage-lacking derivative (a4ΔApp) retained normal liposome binding activity (Figure 3). The a4 mutant vesiculated liposomes without any tubulation, while a4ΔApp lost these membrane-deforming activities (Figure 5D and Supplementary Figure 4). The concave surface-induced membrane deforming activity appeared to be lost in the a4 mutant, while the appendage's membrane insertion remained active. These results suggested that the rigidity of the crescent dimer structure is essential for liposome tubulation but not for vesiculation, although appendage insertion induces the vesiclulation.

Roles for the amphipathic helix 0 of the N-BAR domain

The structure of a short amphipathic helix (helix 0) characterizing the N-BAR (Peter *et al*, 2004) can be resolved in the a4 mutant structure due to its tight crystal packing (Figures 5B and 6). The helix 0 is disordered in the wild type (Figure 6) and the ΔApp structures. The helix 0 has been

©2006 European Molecular Biology Organization

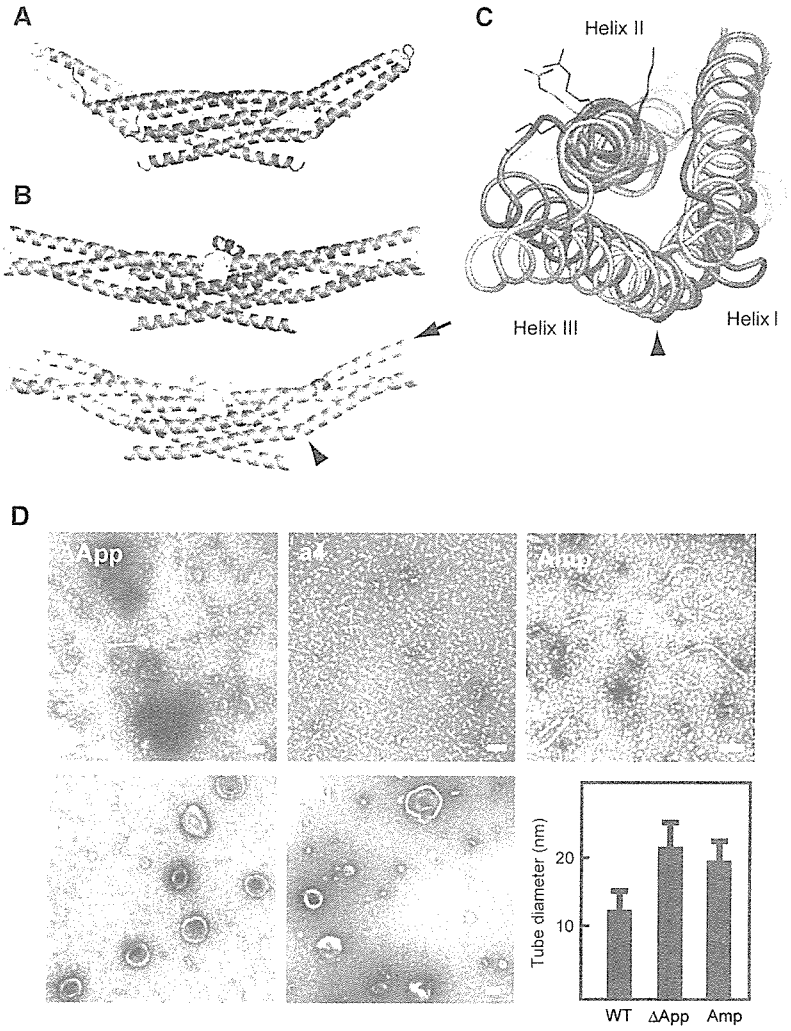

Figure 5 Distinct liposome tubulation induced by endophilin-A1 BAR domain mutants. (**A**) Ribbon representation of a mutated EndA1-BAR dimer lacking the entire appendages (ΔApp, PDB ID: 1X04). The entire appendage (Q59–Q88) was replaced with a helical stretch (AHLSSLLQ) derived from arfaptin2 sequence (A152–Q159, Y155S). Red, mutated segment. (**B**) Ribbon representation of the a4 mutant with swinging arms (PDB ID: 2D4C). One helical pitch was inserted into the helix II in the proximal portion of the extending arm (QSAL was inserted between I154 and Q155). Two dimers in the asymmetrical unit are shown separately. Red, inserted segment; magenta, helix 0. The bending patterns of the helix II and III varies among four monomers. An obvious kink in the helix III remains in the orange monomer (arrowhead, also in (C)). The residual curvature in the blue–green dimer is provided by the intersection of the monomers. (**C**) Superimposition of the a4 mutant monomer (orange one in (B)) and the wild-type monomer (blue) in the core region. A view from the distal end along the helix II (arrow in (B)) shows the maximum structural difference in these arms. Side chains of K171, 173 and R174 are shown. The helix III rotates 12° counterclockwise and shift 6 Å relative to the helix II at the distal end of the arm. The helix 0 and the core region are omitted. (**D**) Negatively stained liposome tubules induced by the BAR domains of endophilin mutants and amphiphysin. ΔApp, 7 μM, incubated for 10 min; a4, 7 μM, 10 min; a4ΔApp, 28 μM, 10 min; ΔNT, 21 μM, 10 min; Amp, 7 μM, 10 min. Note that a4, a4ΔApp, and ΔNT do not induce liposome tubulation. Scale, 100 nm. The bar graph shows tubule diameter (mean and s.d.).

suggested to be helical only when the amphiphysin BAR domain binds to liposomes (Peter *et al*, 2004). The helix 0 displays the hydrophobic branch of T14, V17 and V21 on one side, while K12, K16 and E19 on the other side (Figure 6). The helix 0 is connecting with the Helix I by a flexible linker G23–G24–A25. Consistent with the previous report (Farsad *et al*, 2001), truncation of the helix 0 (ΔNT) resulted in loss of liposome binding activity (Figure 3) and consequently abolished the tubulation (Figure 5D). In contrast, all the helix 0-containing mutants, including the A66D and the a4ΔApp showed intact liposome binding activity irrespective of their tubulation or vesiculation activities. These results indicate that the helix 0 in the endA1-BAR is critical for liposome binding and that the membrane binding of endA1-BAR via helix 0 is not sufficient to induce tubulation or vesiculation.

BAR domain induces tubular membrane deformation in vivo

To explore the significance of the helix 0, the rigid crescent mold, and the appendage of endophilin-A1 BAR domain *in vivo*, we further examined the membrane deformation activity of endophilin-A1 BAR domain in cells (Figure 7). Human umbirical vascular endothelial cells (HUVECs) expressing endophilin-A1 lacking SH3 domain (residues 1–296, hereafter, EndA1-BAR296), which was C-terminally tagged with enhanced green fluorescence protein (EGFP), exhibited intracellular fibrous structure similar to those induced by other BAR domain-containing molecules (Kamioka *et al*, 2004; Itoh *et al*, 2005). Notably, these structures developed from the periphery toward the center of the cells dynamically and disappeared reversibly in living cells (Figure 7E and

©2006 European Molecular Biology Organization